**PhD-Thesis**

# Studies on the Role of Lipoprotein Lipase Mediated Lipotoxicity of Skeletal Muscle and the Effect of Adipose Triglyceride Lipase in the Tumor Metabolism


submitted by

**Tamilarasan Kuppusamy Palaniappan**


for the Academic Degree of

**Doctor of Philosophy**

**(Ph.D.)**

at the


**Medical University of Graz**

Institute of Pathology


Under Supervision of

**Univ. Prof. Dr. Gerald Hoefler, M.D.**

**(2014)**

# Table of Contents

# Zusammenfassung

Der Hauptenergiespeicher bei Tieren sind Adipozyten. Wird Fett außerhalb der dafür vorgesehenen Zellen und Organe gespeichert, beispielsweise in Leber, Herz oder Skelettmuskel, führt dies zu pathologischen Veränderungen wie Fettleber, Kardiomyopathie, nicht-insulinabhängigen Diabetes mellitus und Myopathie; oder kurz zur Lipotoxizität. Das Konzept der Lipotoxizität ist, dass die ektopische Akkumulation von Lipiden in nicht-adipösen Gewebe sich negativ auf die betroffenen Gewebe und Organe auswirkt. Die Auswirkung eines Lipidüberschusses in der Skelettmuskulatur wird nach wie vor diskutiert. Das Enzym Lipoproteinlipase (LPL) erleichtert die Aufnahme von Lipiden in den Muskel. Ein gut geeignetes murines Modellsystem um direkte Auswirkungen des Lipidüberschusses im Muskel zu studieren ist die MCK (m)-hLPL Maus, in derLPL ausschließlich in Skelett- und Herzmuskel exprimiert wird. Um die direkten Auswirkungen des Lipidüberschusses in der Muskulatur *in vivo* und in Zellen *in vitro* zu studieren wurde das MCK (m) h-LPL-Maus-Modell und C2C12 Zelllinien mit hLPL Überexpression verwendet. Die Studien haben gezeigt, dass ektopische Lipidansammlung, wie sie durch hLPL Überexpression verursacht wird, zu vermehrter Apoptose und proteasomaler Aktivität *in vivo* und *in vitro* führt, sowie zu Muskelschäden, welche durch Verlust der körperlichen Leistungsfähigkeit deutlich wurden. Zusätzlich konnte mit Hilfe der Elektronenmikroskopie Läsionen des Muskelgewebes gezeigt werden. Weiters deuten die Ergebnisse auf eine drastische Abnahme des Muskel-Regenerationspotentials *in vivo* hin. Im Einklang dazu konnte ein Verlust des Potentials zur myogenen Differenzierung bei murinen C2C12 Zellen mit hLPL Überexpression gezeigt werden.

Die Lipolyse wurde als ein zentraler Mechanismus des Zellstoffwechsels und Produzent von Signalfaktoren identifiziert. Der Lipidstoffwechsel startet mit der Aufnahme von Lipiden, welche in weiter Folge mit Hilfe der Lipoprotein-Lipase (LPL) zu Fettsäuren hydrolysiert werden und in Form von Triglyceriden (TG) in den Zellen gespeichert werden. Triglyceride werden von einer Gruppe von Lipasen gespalten, wobei die Adipozyten Triglyceridlipase (ATGL) eine wichtige Rolle spielt. ATGL katalysiert die Freisetzung von Fettsäuren (FA), welche von

den Zellen für die Energieerzeugung verwendet werden können. Generell ist der Lipidstoffwechsel essentiell um die normalen Zellfunktionen aufrecht zu erhalten. Ein veränderter Lipidstoffwechsel führt immer abnormer Zellfunktion.
Krebszellen weisen metabolisch veränderte zelluläre Funktionen auf. Hinweise deuten vermehrt darauf hin, dass Krebszellen Änderungen in verschiedenen Aspekten des Fettstoffwechsels zeigen. Inhibitoren wie SB-204990, Acetyl-CoA-Carboxylase (ACC)-Inhibitoren, und Fettsäure-Synthase (FAS)-Inhibitoren greifen in den Fettstoffwechsel ein und ihre Tauglichkeit hinsichtlich Tumormanagement wird derzeit evaluiert. Die Rolle von der ATGL im Rahmen einer malignen Erkrankung ist jedoch noch unklar. Um die Rolle von ATGL in Tumoren zu erforschen, wurden durch Transduktion von bcr-abl in B-Zellen aus dem Knochenmark von Wildtyp (Wt) und ATGL Knockout (ATGL-ko) Tumorzellen hergestellt. Als weiteres Modellsystem wurde ATGL in Lewis-Lungenkarzinom Zellen dauerhaft gehemmt. Die Wachstumseigenschaften der ATGL-ko-Zellen und WT-Zellen wurden *in vitro* als auch *in vivo* untersucht. *In vitro* zeigten ATGL-ko-Zellen vergleichbare Wachstumseigenschaften wie WT-Zellen. Unter der Annahme, dass die ATGL-ko Tumorzellen in den Mäusen lipotoxische Effekte zeigen, die zu einer Hemmung des Tumorwachstums zu führen, wurden ATGL-ko und WT-Zellen in Mäuse injiziert um das Tumorwachstum zu untersuchen. Unerwarteter Weise formten die ATGL-ko Tumorzellen größere Tumore als die Wt Zellen, was darauf hinweist, dass ATGL, neben der Hauptfunktion der Lipolyse auch eine wichtige Rolle beim Tumorwachstum spielt.Diese Ergebnisse konnten durch Studien mit immunsupprimierten RAG2-gamma und RAG2-Mäusen bekräftig werden, wo wiederum ATGL-ko-Zell-Tumore schnelleres Wachstum zeigten. Zusätzlich haben neue Studien gezeigt, dass Fenofibrat (ein PPAR alpha Agonist) enthaltendes Futter das Tumorwachstum von B-Zellen in Mäusen hemmt.

Zusammenfassend kann gesagt werden, dass diese Forschung auf dem Gebiet des Lipidstoffwechsels in Bezug auf Lipotoxizität gezeigt hat, dass Lipidüberschuss durch LPL im Skelettmuskel erhöhte Toxizität verursacht, welche zu schlechtem Skelettmuskelzell-Wachstum führt, und dass eine Inhibierung der ATGL zu erhöhtem Tumorwachstum in Mäusen führt. Basierend auf diesen Beobachtungen schlussfolgern wir, dass Lipidüberschuss, verursacht durch hLPL,die physiologische Funktion auf unterschiedliche Weise verändern kann, und

dass die ATGL, welche hauptsächlich in der Lipolyse eine Rolle spielt, auch andere Funktionen, im Zusammenhang mit dem Tumorstoffwechsel, haben könnte. Der genaue Mechanismus muss jedoch noch untersucht werden.

## Summary

The main energy storage sites of animals are their adipocytes. If fat is stored ectopically, for example in liver, heart, or skeletal muscle it induces pathological changes such as fatty liver, lipid cardiomyopathy, non-insulin dependent diabetes mellitus, and skeletal muscle myopathy, or in short lipotoxicity. The concept of lipotoxicity is that the ectopic accumulation of lipids in non-adipose tissue leads to negatively affects cells, tissues and organs that store it. It is not clear whether the fat stored ectopically in muscle is lipotoxic. The enzyme Lipoprotein lipase (LPL) facilitates entry of lipids into the muscle. An intriguing murine model system to study direct effects of lipid overload in muscle is the MCK(m)-hLPL mouse where LPL is expressed exclusively in skeletal and cardiac muscle. The MCK(m)h-LPL mouse model and C2C12 cell-lines overexpressing hLPL were used to study the direct effects of lipid overload in muscle *in vivo* as well as in muscle satellite cells in culture. The studies showed that ectopic lipid accumulation was caused by hLPL over expression lead to enhanced apoptosis and proteasomal activity *in vivo* and *in vitro* as well as marked muscle damage as evidenced by loss of physical performance. In addition, results of electron microscopically observation of skeletal muscle indicated the presence of visible lesions. Moreover, the studies indicated a drastic decrease in muscle regeneration potential *in vivo*, which was also evidenced by a loss of myogenic differentiation potential of C2C12 murine satellite cells upon over expression hLPL.

Lipolysis has been identified to be a central mechanism of cell metabolism and a producer of many signaling factors. Lipid metabolism starts from the uptake of lipids in the form of fatty acids by lipoprotein lipase, and lipids are stored as triglyceride in the cells. Triglycerides can be cleaved by a group of enzymes called lipases of which one of the major enzymes is Adipose Tri-Glyceride Lipase (ATGL) leading to the release of fatty acids that can be used by the cells for energy production. In general, metabolism of lipids is important to maintain normal cell metabolism. Altered lipid metabolism always results in abnormal cellular function. Cancer cells also show metabolically altered cellular function. Increasing evidence indicates that cancer cells show alterations in different aspects of lipid metabolism. There are inhibitors like SB-204990, acetyl-coA carboxylase (ACC) inhibitors, and

fatty acid synthase (FAS) inhibitors targeting the lipid metabolism that are emerging as anticancer strategies. However, the role of ATGL in the course of malignant diseases is unclear. To explore the role of ATGL in tumors, wild type (Wt) and syngeneic ATGL knockout (ATGL-ko) tumor cells were created by transducing p185bcr-abl in B-cells derived from bone marrow of Wt and ATGL-ko mice respectively. In addition, ATGL of Lewis lung carcinoma cells (LLC) was permanently inhibited by stable expression of pre-miRNA which could target the ATGL. The growth characteristics of the ATGL-ko cells and Wt cells were studied *in vitro* as well as *in vivo*. ATGL ko B-cells showed growth characteristics similar to the one of Wt cells when cultured *in vitro*. The ATGL-ko and Wt cells were injected into the mice, and analyzed for the tumor growth. The expected observation would have been that the Atgl-ko tumor cells in the mice exhibit lipotoxic effects which lead to inhibition of the tumor growth, but the Atgl-ko cells formed even bigger tumors than the Wt cells in the mice indicating that ATGL may play a potential role in the tumor growth apart from its major function of lipolysis of lipids. In addition, studies of Atgl-ko cell growth in immune suppressed RAG2–gamma mice and RAG2-mice strengthened the result that the Atgl-ko cell tumors grow larger. The difference, however, is less pronounced since Wt tumors grow bigger in immune suppressed mice compared to Wt mice. Furthermore, recent studies showed that B-cell lymphoma is suppressed in mice fed with fenofibrate (PPAR alpha agonist) supplemented food, due to modulation of the lipid metabolism. However the results related to ATGL knockdown indicated that the ATGL-ko cells show growth advantage compared to Wt cells *in vivo.*

In summary research related to lipid metabolism with respect to lipotoxicity indicated that skeletal muscle overload of lipids by hLPL caused increased toxicity leading to poor growth of the cells which causes the altered physical performance, and the lipid metabolism related to the cancer indicated that the inhibition of ATGL leads to increased tumor growth in mice. Based on these observations I conclude that overload of lipids by hLPL can alter the physiological function according to the concept of lipotoxicity but that ATGL might have other functions in the context of tumor metabolism which have to be studied further.

# Abbreviations

| | |
|---|---|
| ABL | Abelson |
| ACC | Acetyl-CoA carboxylase |
| ACL | ATP citrate lyase |
| ATGL | Adipose triglyceride lipase |
| Atgl-ko | Adipose triglyceride lipase knockout |
| ATP | Adenosine-5'-triphosphate |
| B-ALL | B-Acute lymphoblastic leukemia |
| BCR-ABL | anoncogene of BCR and ABL |
| CCK | Cholecystokinin |
| cDNA | complementary DNA |
| Chok | Choline kinase |
| CML | Chronic myelogenous (or myeloid) leukemia |
| CTX | Cobra toxin |
| DMEM | Dulbecco's Modified Eagle Medium |
| EDTA | Ethylene di amine tetra acetic acid |
| EGTA | Ethylene glycol tetra acetic acid |
| ELMI | Electron microscopy |
| FASN | Fatty acid synthase |
| FBS | Fetal bovine serum |
| FFA | Free fatty acid |
| GFP | Green fluorescent protein |
| HCL | Hydrogen chloride |
| HEPES | N-2-hydroxyethylpiperazine-N'-2- ethane sulfonic acid |
| hLPL | Human Lipoprotein Lipase |
| HS | Donor Horse Serum |
| HSL | Hormone sensitive lipase |
| IHC | Immuno-histochemical detection |
| LDs | Lipid droplets |
| LLC | Lewis lung carcinoma cells |
| LLC-Atgl-kd | Lewis lung carcinoma cells with ATGL knock down |
| LLC-Wt | Lewis lung carcinoma cells with wild type cells |
| LPL | Lipoprotein lipase |
| LPL-OV | Lipoprotein lipase over expression |
| LUC | Luciferase |
| m. gast | *musculus gastrocnemius* |
| m.sol | *musculus soleus* |
| MCK | Muscle keratine kinase |

| | |
|---|---|
| MG | Monoacylglycerols |
| MGL | Monoacylglycerol lipase |
| mRNA | messenger RNA |
| Myf5 | Myogenic regulatory factors five |
| MyoD | Myoblast determination protein 1 |
| P/S | Penicillin/Streptomycin |
| PCR | Polymerase chain reaction |
| PET | Positron emission tomography |
| PZ | Panceozymin |
| PZ-CCK | Pancreozymin-cholecystokinin |
| qPCR | Quantitative real time polymerase chain reaction |
| RLU | Relative luciferase units |
| RNA | Ribonucleic acid |
| RPMI | Roswell Park Memorial Institute |
| Sh RNA | scrambled RNA |
| TG | Triacylglycerol |
| VLDL | Very low density lipoproteins |
| Wt | Wild type |

# Introduction

## *Lipid metabolism and transport*

### Lipoproteins

The living organism is exposed to many cycles of over and under-nourishment due to changing of environmental conditions. In order to adopt these settings, organisms developed various means to store energy in the cells and tissues. One of the major forms of energy storage is lipids. Lipoproteins (LPs) are the transporters of fat and cholesterol in the body. The liver, adipose tissue (AT), and skeletal muscle play an important role in lipid homeostasis which leads to pathological lipid accumulation. The basic components of the LPs are proteins, cholesterol, phospholipid, cholesterol-ester and triacylglycerol (TG). In addition, the LPs are surrounded by a lipid layer. The proteins which are present in the lipid layer are called apolipoproteins (apo), some of the proteins are integrated, and some proteins are peripheral. The LPs are classified into chylomicrons (CM), intermediate lipoproteins (IDL), very low density lipoproteins (VLDL), low density lipoproteins (LDL), and high density lipoproteins (HDL). The CM and the VLDL contain rather high amounts of TG compared to other LPs. Therefore, they are sometimes called triglyceride rich LPs. The integrated protein in the LPs is used as a marker to identify their specificity. The integrated protein of CM is apoB-48, the integrated protein of IDL, VLDL, as well as LDL is apo-100, and the apoA1 is used as a marker of HDL (Welty *et al.*, 2004). Other receptors of LPs, which are also involved in the lipid transport-related signaling, are apoC and apoE, etc. (Figure 1). The TG carried inside the LPs is composed of one glycerol and three fatty acids (FA). TG and cholesterol ester are transported to tissues by LPs

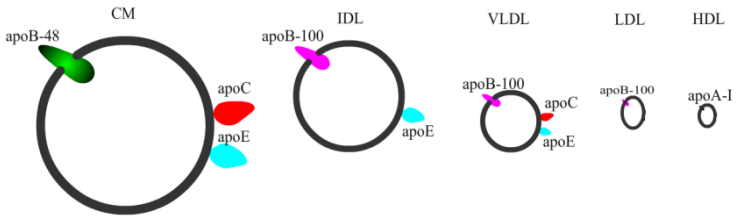


Figure 1 Lipoproteins.

## Lipid transport from the food to blood

In general, fat is ingested as part of the normal diet. As a first step, it is mixed with various digestive enzymes during the transport from the mouth to small intestine. The duodenum is a part of a small intestine where the main activity of fat hydrolysis as well as absorption occurs in the body. The schematic diagram represents the outline of a lipid transport from the food to the bloodstream (Figure 2). Initially, FAs in the duodenum stimulate a peptide hormone called cholecystokinin-pancreozymin. Afterwards, the cholecystokinin (CCK) causes the gallbladder to secrete bile acid to the intestine. The pancreozymin activity leads to the release of other digestive enzymes and pancreatic TG lipase. Furthermore, the pancreatic lipase hydrolyzes the TG to fatty acids (FA) and 2-monoglycerides. At this stage, short chains FAs enter the portal vein, and reach the liver. However, the long chains FAs are re-esterified with 2-monoglycerides to form CM. These CM enter the lymphatics and then quickly reach the blood stream (Young *et al.*, 2013).

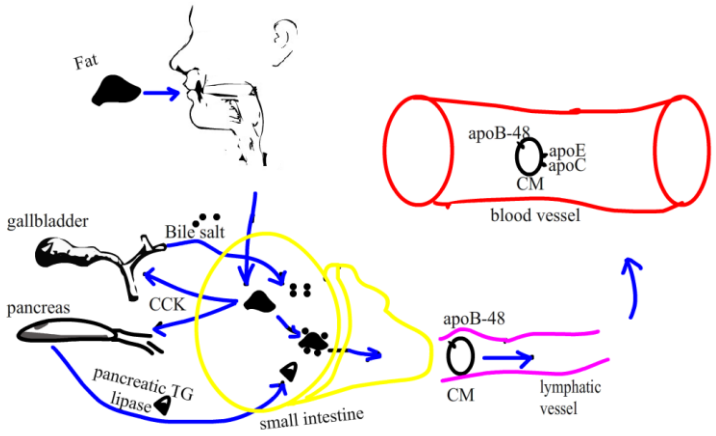


**Figure 2 Schematic diagram depicting the transport of fat from food to the blood.**

## Lipid transport in to the muscle

The CM, which is synthesized during the process of lipid transport, contains TG and cholesterol ester for the transport to a muscle. Integrated protein called apoB-48serves as a marker for the CM. When CM enters the bloodstream, the peripheral proteins apoC and apoE join prior to the transport of lipids. Through the bloodstream, the CM reaches the tissues of various organs like adipose tissue, skeletal muscle, iver, etc. The liver absorbs the CM by interacting with one of its specific receptor to the apoE of the CM. The liver also could synthesis the TG upon various stimulations by multi enzyme complex called fatty acid synthase. Initially, the acetyl-coA is converted to FA. The FA esterified with glycerol leads to generate TG. The liver and the adipose tissue are the major TG controllers of the body. The schematic diagram indicates the outline of CM uptake as well as TG synthesis in the hepatocyte as well as the release of VLDL. The liver secretes VLDL, which serves to redistribute TG to adipose tissue, heart and muscle (Young *et al.*, 2013) (Figure 3). When the VLDL reaches the blood, apoC and apoE join for the transport of its lipids to the tissues. Lipoprotein lipase (LPL), cleaves the VLDL, and releases the FAs to the tissue. Furthermore, after release of the FAs to the tissue, VLDL is converted into IDL and LDL. The schematic diagram shows the outline of LPs transport to tissue (Figure 4). Increase in the LPL activity is one of the major initial processes to the lipid overload to the cell.

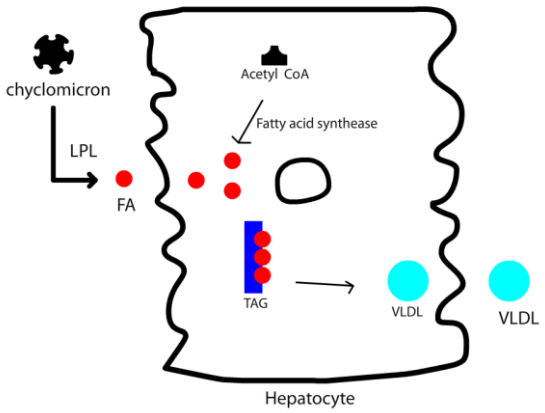


**Figure 3 Schematic diagram indicates the outline of CM uptake as well as TG synthesis in the hepatocyte, and the release of VLDL.**

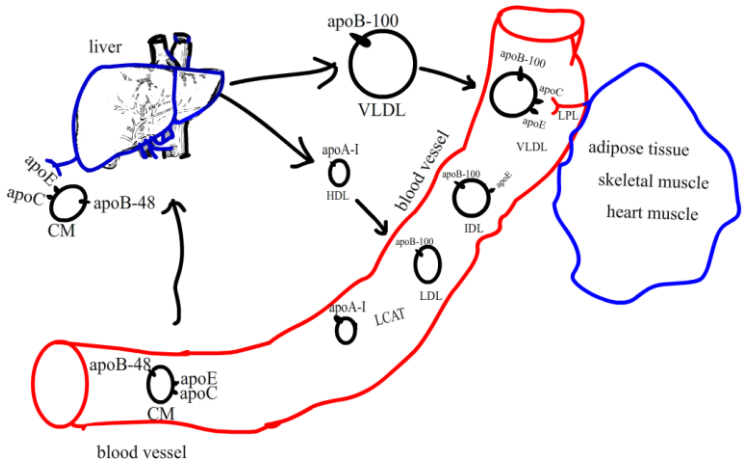


**Figure 4 Schematic diagram indicates the outline of LPs transport to tissue.**

## *Lipotoxicity*

The ectopic lipid accumulation leads to toxic effects called lipotoxicity (van Herpen *et al.*, 2008).The lipids are transferred from the food to the cells through LPs, and stored as TG in adipose tissue (AT). Only AT has the ability to secrete FFAs into the circulation. The capacity of AT to expand appropriately when lipid storage is needed is limited for a given individual. Hence, when the limit is exceeded, the lipids begin to accumulate in ectopic tissues causing metabolic dysfunction and insulin resistance due to lipotoxic effects (Nielsen *et al.*, 2014). Ecotopic fat leads to cardiometabolic and vascular risk (Lim *et al.*, 2013).Neutral lipid is most likely not lipotoxic. However, cellular neutral lipid content can be understood as a good measure for lipid overload. Other lipid species such as free fatty acids (FFA) are more likely to cause lipotoxicity. Lipid droplets in the muscle tissue can be visualized by using magnetic resonance spectroscopy or by various microscopic methods applied to tissue sections like oil-red-O staining. Lipid droplets are detectable in skeletal muscle, and they often occur in the proximity of mitochondria, but their size and number are variable. The continuous physical resistance training has a positive effect on intra-muscular lipid droplet content. However, this lipid measure is decreased right after physical training. It was suggested that lipid droplets are a source of fuel for the muscle. In skeletal muscle and liver, lipid accumulation has been associated with the development of insulin resistance, which is an early hallmark of developing type 2 diabetes mellitus. More specifically, accumulation of intermediates of lipid metabolism, such as diacylglycerol (DAG) and Acyl-CoA have been shown to interfere with insulin signaling in these tissues (van Herpen *et al.*, 2008). In addition, a high caloric intake eventually often leads to the metabolic syndrome, and also enhances the formation of intra muscular lipid droplets (van Herpen *et al.*, 2008). There are many studies showing that an alteration of the LPs-level and its interaction cause many diseases. The alteration in the apo metabolism also causes chronic kidney diseases, metabolic syndrome, etc (Batista *et al.*, 2004). Adipocytes do not only store energy as a lipid, but also do inform the brain and the muscle tissue about the energy storage status by excreting leptin which acts on the hypothalamus. Leptin leads to suppression of the caloric intake of lipids as well as stimulation of the lipid-beta-oxidation in the muscle (Pelleymounter *et al.*, 1995; Shimabukuro *et*

*al.*, 1997; Zhou *et al.*, 1997). Humans with generalized lipoatrophy, such as fatty liver, lipid cardiomyopathy, non-insulin dependent diabetes mellitus and insulin resistance, as well as skeletal muscle myopathy conditions directly feed into the concept of lipotoxicity i.e., the ectopic accumulation of lipids in non-adipose tissue destroys the organs (Lee *et al.*, 1994).

## *Lipid and skeletal muscle*

An excellent model system to study direct effects of lipid overload in muscle has been established earlier by Levak-Frank (Levak-Frank *et al.*, 1995). A fully functional human LPL (hLPL) minigene was expressed exclusively in skeletal and cardiac muscle using the muscle specific promoter of muscle keratine kinase (MCK). Three independent transgenic mouse lines were generated that express hLPL at low, medium, or high levels (hLPL-MCK l, m, and h, respectively) and there was a dose dependent decrease in plasma triglyceride levels, elevation of FFA uptake by muscle tissue, weight loss, leads to the premature death. The mice showed severe myopathy, fiber atrophy, enhanced glycogen storage, mitochondrial and peroxisomal proliferation (Levak-Frank *et al.*, 1995). Several other groups used this mouse model, and it was found that in muscles of these mice alpha-tocopherol levels (Sattler *et al.*, 1996) and intracellular FFA(Hoefler *et al.*, 1997), as well as intramuscular TG levels (Voshol *et al.*, 2001) were increased. Furthermore, the peroxisomal enzymes were induced (Hoefler *et al.*, 1997). In addition, no inhibition of insulin-stimulated whole-body and muscle-specific glucose uptake could be detected (Voshol *et al.*, 2001).

## *Lipid and tumor*

Alteration of lipid metabolism have been recognized as a hallmark of cancer cells (Notarnicola *et al.*, 2014). Cancer cells metabolically adopt to undergo cellular proliferation. Lipids, besides their well-known role as energy storage, represent the major building blocks for the synthesis of neo-generated membranes. There is increasing evidence that cancer cells show specific alterations in different aspect of lipid metabolism (Lettieri Barbato *et al.*, 2014; Swinnen *et al.*, 2006), and elevated glucose transport with increased rates of glycolysis (Young *et al.*, 2008). Hyperlipidemia is the most prominent sign of altered lipid metabolism in the tumor and cancer associated cachexia, which is a devastating syndrome common in many types of cancer. Moreover, it frequently involves an impairment of body lipid and cholesterol metabolism (Costelli *et al.*, 1999).The inhibition of the following enzymes from the fatty acid synthesis by chemical, as well as shRNA inhibitors showed inhibition of cancer cells: (i) ATP citrate lyase (ACL) inhibition by RNAi or the chemical inhibitor SB-204990 limits *in vitro* proliferation and survival of tumor cells (Bauer *et al.*, 2005; Hatzivassiliou *et al.*, 2005). (ii) Acetyl-CoA carboxylase (ACC) is the most highly regulated enzyme in the fatty acid synthesis(Wakil *et al.*, 2009). The shRNA inhibition of ACC1 induces the apoptosis in breast cancer (Chajes *et al.*, 2006) as well as prostate cancer (Brusselmans *et al.*, 2005). (iii) Fatty acid synthase (FASN) inhibition causes inhibitory effect of ovarian cancer growth in SCID mice (Wang *et al.*, 2005). (iv) The choline kinase (Chok) inhibition reduces the phosphomono esters in cancer xenografts (Al-Saffar *et al.*, 2006). A recent study reported that the hydrolysis of monoacylglycerol (MG) might be a source of FAs in tumor cells, and that the synthesized FAs are immediately converted into TG.MGL is highly expressed in aggressive human cancer. Moreover, MGL activity plays a major role in the signaling of lipids which leads to the stimulation of tumor cells in an autocrine manner in order to promote their survival, migration, and invasion (Nomura *et al.*, 2010). The lipid metabolism related to the lipolysis and tumor is not fully understood. Therefore, inhibition of ATGL as well as HSL may help to prevent cancer-associated cachexia (Currie *et al.*, 2013).

Leukemia is a type of cancer of white blood cells. The white blood cells originate from the bone marrow. Because of the various types of white blood cells, leukemia is classified based on the origin of the precursor cells. Lymphoid precursor cells (blasts) give rise to B-lymphocytes and T-lymphocytes. Lymphoblastic leukemia is a cancer originating from B- precursor cells and characterized by circulating B-blasts. The nodal (tumor forming) variant is called lymphoblastic lymphoma. Both are characterized by very rapid growth leading to death within a few weeks if untreated.

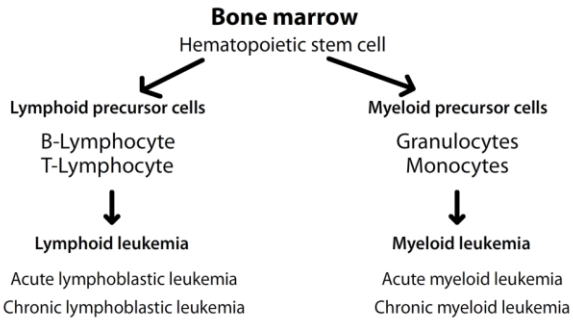


**Figure 5 Types of leukemia based on the origin of precursor cells.**

DNA mutations cause normal bone marrow cells to become leukemia cells. Oncogenes are characterized by gain-of-function mutations of normal regulatory genes or proto-oncogenes, and these oncogenes contribute to human cancer formation by supporting accelerated proliferation, de-regulating cell cycle control or blocking apoptosis (Todd *et al.*, 1999). Translocation describes a process where DNA from one chromosome breaks off and becomes attached to a different chromosome. Translocations are the most common type of DNA change that lead to leukemia. The most common translocation in B-cell leukemia in adults is known as the *Philadelphia chromosome* (Ph chromosome), which is a translocation of DNA between chromosomes 9 and 22, abbreviated as t (9;22) (Gleissner *et al.*, 2002; Mishra *et al.*, 2006). More than 95% of patients with chronic myeloid leukemia (CML) have a BCR-ABL translocation in their leukemia cells (Melo, 1996). During translocation, the ABL gene located on chromosome 9,which contains the Abelson (ABL) kinase domainis moves to chromosome 22 to join with a specific break point cluster region (BCR) to form the BCR-ABL gene. Figure 6 indicates the schematic

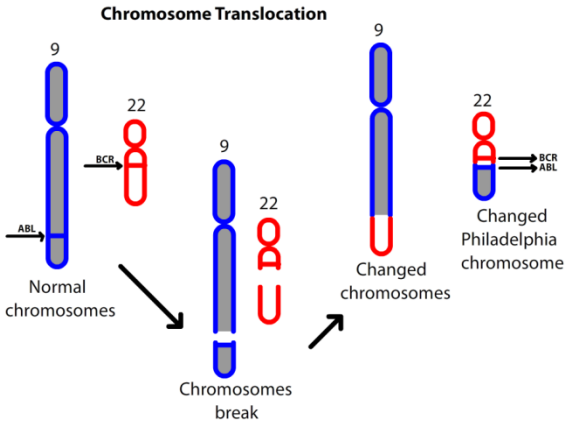


**Figure 6 schematic diagram of chromosome translocation.**

diagram of chromosome translocation, which leads to the formation of the BCR-ABL gene in chromosome 22. The newly formed BCR-ABL encodes for an oncoprotein (Raponi *et al.*, 2009).

BCR-ABL fusion proteins are of different sizes p190, p210 and p230, depending on the site of breakpoint within the BCR gene (Raponi *et al.*, 2009). There are three mRNA transcripts e1a2, e13a2 and e14a2 and several atypical ones which have been observed (Melo, 1996). The BCR-ABL translocations may also occur in acute lymphoblastic leukemia (Raponi *et al.*, 2009), and are associated with an aggressive course of disease. There is increasing evidence that lipid metabolism is involved in cancer growth (Lettieri Barbato *et al.*, 2014). Managing lipid metabolism in proliferating cells is a new perspective for cancer therapy (Lettieri Barbato *et al.*, 2014). Alterations in the lipid metabolism were detected in the cancer cells (Notarnicola *et al.*, 2014). The role of ATGL and cancer proliferation is unclear (Currie *et al.*, 2013).

# Hypothesis

## *Overview of hypothesis*

In general, LPL hydrolyses VLDLs and CM from the blood stream (Mead *et al.*, 2002) at the surface of capillary endothelium which leads to the release of FAs to the cells. FAs are subsequently taken up by tissue (Busquets *et al.*, 2001; Lecker, 2003).FAs are used in the mitochondria to release ATP as energy source for the cells by a process called beta-oxidation. The excess of FA esterifies with glycerol, and it is stored as TG in the cell. When the cell needs energy, the TG will be hydrolysed by the enzymes ATGL, HSL, and MGL that leads the release of FAs. The schematic diagram represents the VLDL uptake by the cell, and the release of FAs by various enzymes (Figure 7).The FAs enter in to the beta-oxidation process, and serve to produce energy. Alternatively, the lipids could be stored in the cells. Excess of lipids stored in the cells can cause damage to the cells, which is then called lipotoxicity. There are two approaches to study the lipotoxic effects by increasing lipid storage in the cell. One possibility is the over expression of LPL in the cells which may increase lipid levels in a way that harms the cells that can be analysed and studied. Another possibility is to inhibit the ATGL in cells which might also lead to increased intracellular TG levels as well as altered FAs-mediated signalling thus might damage the cells. The increased LPL in the skeletal muscle, and the another possibility of inhibited ATGL in cancer cells were the main approaches focused on in these studies.

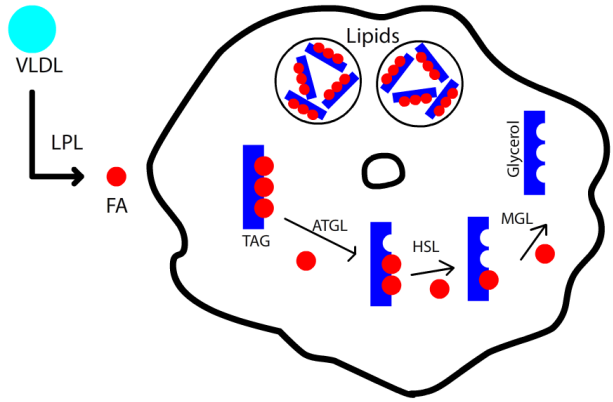


**Figure 7 Schematic diagram of lipid intake and breakdown of a cell.**

## *Hypothesis approach*

Overload of lipid might cause damage to the cells. One possible mechanism for excess lipid could be caused by the enzyme LPL. Therefore, the first aim of the study is to understand the effects of lipotoxicity by LPL over expression in the skeletal muscle. Other possible mechanism of inhibiting ATGL related to cancer is not yet studied. Therefore, the other aim of the study is to understand the role of inhibited ATGL in cancer cells.

**MCKM mice were used to analyze**

i. Physical performance (running capability by using treadmill).
ii. Skeletal muscle regeneration (damage the skeletal muscle by toxin, and study the recovery by H&E staining of muscle tissue section)
iii. Parameters of the skeletal muscle like
    a. Apoptosis
        - Tunnel staining
        - ATP dependent proteasomal enzymatic activity assay
        - caspase3/7 enzymatic activity assay
        - Active caspase3 by IHC assay
    b. FA, TG levels.
    c. Electron microscopic structure of skeletal muscle

**Stable over expression of h-LPL in C2C12 cells was used to analyze**

i. Myogenic differentiation
ii. Expression of Myo-D by IHC
iii. Lipid droplet formation by staining using nile red and bodipy

**Regulated expression of h-LPL in C2C12 cells was used to analyze**

i. h-LPL expression,
ii. Myogenic differentiation potential,
iii. TG concentration.

Wt, Atgl-ko,RAG2, and RAG2-gamma mice were used to analyze the tumor growth in the following setting

i. Mice were injected with the Atgl-ko and control cancer cells. Tumor analysis was performed after the same period of time post-injection.

ii. Wt mice were injected with the Atgl-ko and Wt cancer cells. Endpoint of the experiment was chosen in a way to achieve the same tumor weight. Gene expressions were analyzed using an Affymetrix chip.

# Methods

Methods are partially reused from the publication(Tamilarasan *et al.*, 2012) with modifications. The material is reproduced with the permission of Nature Publishing Group.

## *Animal care and use*

Mice C57Bl/6J × CB and isogenic MCK(m)-hLPL mice were maintained on a regular light-dark cycle of 12 hours light and 12 hours dark with a laboratory chow diet with 4.5% w/w fat (Levak-Frank *et al.*, 1995). The MCK(m)-hLPL and Wt mice were bred to develop a minimum number of littermates to study the lipotoxic effects on skeletal muscle. Genotyping of the mice was done by polymerase chain reaction (PCR) from DNA isolated from their tail tissue. Male mice were used for the studies. All mice experiments were performed according to the animal protocol BMWF-66.010/0110-II/3b/2010, as approved by the Austrian government.

The DNA was isolated from the tail tip of each mouse independently with the DNeasy Blood and Tissue kit from QIAGEN. The PCRs were performed using primer sequences amplifying the human lipoprotein lipase (sequences given in table below) and the Multiplex PCR Kit (QIAGEN) with the amount of DNA suggested in the protocol. The PCR products were analyzed by common gel electrophoresis.

**PCR Primers**

| | | | |
|---|---|---|---|
| Human LPL | hLPL | forward | 5'-CCAGTGAGCAAGTCAGCCCT-3' |
| | | reverse | 5'-ATGACAGGTGCCACGGACT-3' |

## *Physical performance of mice using treadmill experiments*

The physical performance in terms of endurance capacity of six month old MCK(m)-hLPL and Wt control mice were measured with their running capability on a motorized treadmill (IITC Inc./Life Sciences, Woodland Hills, CA, USA). Healthy mice were exercised on a motorized treadmill. Prior to the experiments all the mice had been familiarized to the treadmill by training the mice to run for five minutes at 14 m/min and 0°- degree slope for two days. The treadmill experiments were performed between 9am to 11 am. The physical endurance of mice was assessed

on a motorized treadmill set to a speed of 14 m/min and 0°- slope. A mild electrical stimulus of 100–120 V; 2 mA was applied to the mice when it reaches the rear end of the treadmill lane. The physical performance of the mice was calculated by the value of time in seconds until the mouse receives 10 stimuli.

## *Muscle sample isolation*

MCK(m)-hLPL and Wt control mice were anaesthetized using 3% isoflurane and sacrificed by cervical dislocation. The three different skeletal muscles, Musculus gastronomies (m.gast), Musculus quadriceps (m.quad) and Musculus soleus (m. sol) were anatomically isolated. The muscles were frozen in liquid nitrogen untilfurther analysis.

## *RNA isolation and qRT-PCR*

Total RNA was extracted from the m.gast using Trizol-reagent (Trizol LS reagent, Invitrogen LTD, Paisley, UK). The cDNA was synthesized from RNA (1µg) of the m.gast of MCK(m)-hLPL and control mice withthe “High Capacity cDNA Reverse Transcription Kit (Applied Biosystems, Carlsbad, CA) according to the manufacturer’s protocol. The cDNA-samples (5µl of a 1:20 dilution) were used in triplicates for estimating the mRNA expression of the human LPL gene with real time qPCR. The primers indicated below were designed for qPCR to yield an exon-spanning product of 50 to 90 base-pairs (Heid *et al.*, 1996). The freely available software “Primer 3” (http://frodo.wi.mit.edu/primer3/) (Rozen *et al.*, 2000) as well as other freely available software called as “Oligocalc” (http://www.basic.northwestern.edu/biotools/oligocalc.html) was used to design the primers. The Applied Biosystems (Carlsbad, CA) 5700 Sequence Detection System was used for quantitative PCR together with the SYBR® Green PCR Master Mix from Invitrogen (Calsbad, CA). The temperature profile used for amplification was in-line with the manufacturer’s instructions. The comparative CT method was used for calculating relative gene expression using 18s as reference gene (Livak *et al.*, 2001).

**qPCR Primers**

| | | | |
|---|---|---|---|
| Human LPL | hLPL | Sense | 5'-GTCACGGGCTCAGGAGCATT-3' |
| | | antisense | 5'-ACAGGATGTGGCCCGGTTTA-3' |
| 18s Ribosome | 18s | Sense | 5'-GTAACCCGTTGAACCCCATT-3' |
| | | antisense | 5'-CCATCCAATCGGTGTGCG-3' |

## *Skeletal muscle weight estimation*

The body weight of the mice was measured before the isolation of the skeletal muscle. The whole freshly isolated muscles (m.gast, m.sol and m.quad.) from the MCK(m)-hLPL and Wt control mice were weighed. The weight of the m.gast, m.sol and m.quad were estimated per its body weight.

## *Electron microscopy of tissue section*

Fresh muscle tissue from m.gast as well as m.sol of MCK(m)-hLPL and control mice were cut into small pieces of around 2mm thickness. They were fixed by using a solution containing 2.5% glutaraldehyde in 0.1M sodium-cacodylate buffer with pH 7.3. The fixed muscle samples were contrasted with a solution of 1% osmium-tetroxide in cacodylate, dehydrated and embedded in epoxy-resin. The fixed, embedded muscle tissue was cut by an "Ultracut"-microtome to get sections of a thickness around 1µm.The muscle sections were stained withazure2-dye and methylen (1:1, v:v). The sections of muscle containing areas of interest were cut with a diamond-blade mounted microtome resulting in ultra-thin sections of thickness around < 100nm. To augment the contrast, a treatment with 4% uranyl-acetate in 70% methanol and subsequently lead-citrate was applied, as described by (Venable *et al.*, 1965). The EM image was taken with a Philips CM 100 electron microscope (Philips, Eindhoven, Netherlands).This experiment was performed and analysed by Hannes Temmel from the group of Univ. Prof. Dr. Gerald Hoefler, Institute of Pathology at Medical University of Graz.

## *Determination of FFA and TG*

The lipids were extracted from the tissue homogenate of m.gast. of MCK(m)-hLPL and the control mice by hexane isoproponal method (Hara *et al.*, 1978). The chloroform phase containing neutral lipids was dried with nitrogen gas. Each lipid pellet was solubilised in a solution of 2% Triton X-100 by sonication. FFA were

quantified with the NEFA-HR(2) kit (Wako Chemicals GmbH) as per manufacturer's instruction, and the TG was measured with the Triglyceride FS kit (DiaSys Diagnostic Systems, Holzheim GER) according to the manufacturer's instructions (Hara *et al.*, 1978).

## *Skeletal muscle regeneration*

The muscle injury was triggered to the m.gast of 6-month-old MCK(m)-hLPL and Wt mice by direct injection of 25 µl of 10 µM CTX (Sigma-Aldrich, Vienna, Austria).

The control mice were injected with PBS (Sham) to both groups. To study the wound coagulum, mice were anaesthetized, and the whole m.gast was isolated on the 4th day after injection. The muscle tissue was analyzed to confirm the muscle damage. After 10 days the other groups of mice from the same experiment with CTX and Sham injected were anaesthetized and killed by cervical dislocation. Muscles were carefully anatomically isolated for histological analysis of injury and muscle regeneration(d'Albis *et al.*, 1988; Horsley *et al.*, 2004).The skeletal muscle from the MCK(m)-hLPL mice and the control mice were analysed by histochemistry to study muscle fiber composition (Charge *et al.*, 2004).The muscles were fixed using 4% neutral buffer formaldehyde (formalin). Whole transversal sections of muscles were prepared, and stained with hematoxylin and eosin (H&E) staining. Myogenic regeneration can be characterized by the activation of myogenic cells to proliferate, differentiate, and develop new fiber. The regenerating fibers are characterized by their small calibre and their centrally located myonuclei. Images of H&E-stained transversal sections of muscle myofibers were captured by digital microscopy. The whole transverse sections of each muscle were analyzed for muscle regeneration by centrally nucleated fibers. Cross section area (XSA) of 100–260 myofibers within a fixed area of regeneration (289319 µm$^2$) was measured. This data was analysed by pathologist Dr. Wael Alzoughbi from the group of Univ. Prof. Dr. Gerald Hoefler, Institute of Pathology at Medical University of Graz.

## *Apoptosis estimation*

### Tunel staining

The tunel staining was used to detect apoptotic nuclei in frozen transverse sections of muscle from the m.gast of MCK(m)-hLPL and Wt mice. Themuscle cross sections were stained with the Fluoresce in *In Situ* Cell Death Detection Kit (Roche-Applied-Science, Vienna, Austria) according to the manufacture's protocol. The slides were further counterstained with Alexa Fluor 594 Phalloidin for labeling of actin filaments (1:1000) and DAPI (1:1000) for the nuclei(both from Life Technologies, Vienna, Austria). The slides were visualized using an Olympus BX51 fluorescent microscope equipped with a digital camera DP71. The images of the whole transverse sections were analyzed with cell D software, (Olympus,Vienna, Austria).

### Immunohistochemistry of active caspase3

Skeletal muscle of each mouse was carefully isolated from the m.gast of MCK(m)-hLPL and the control mice were fixed with a solution contain 4% buffered formalin and embedded in the paraffin. The IHC of the muscle samples were performed on paraffin sections of the muscle samples using the anti-active caspase3 antibody (AF 835,R&D Systems, Minneapolis, MN). Nuclei were counter stained using haematoxylin. The appropriate secondary antibody is given in the table below.This experiment was performed by Silvia Schauer from the group of Univ. Prof. Dr. Gerald Hoefler, Institute of Pathology at Medical University of Graz.

| Tissue or cells | Primary antibody | Dilution | Antigen retrieval | Incubation & detection | Negative control |
|---|---|---|---|---|---|
| FFPE - formalin fixed paraffin embedded material | Polyclonal rabbit antibody to Active Caspase 3 (R&D Systems) | 1:25 | 0.01M Sodium-citrate buffer pH 6.0 for 40min | Incubation with DAKO REAL EnVision+ Detection system (K4061) | Omission of the primary antibody |
| Formalin Fixedcells | Monoclonal mouse antibody to Myosin Skeletal Muscle heavy chain (M9850-15B, US Biological) | 1:100 | 2% TritonX100 10min | Incubation with anti-mouse-Alexa488 antibody, A11001, Invitrogen (1:500) | Omission of the primary antibody |

### Biochemical caspase

Frozen muscle tissue of the m.gast fromMCK(m)-hLPL and control mice were weighed about 15 to 25mg. Each transversal muscle was homogenized on ice with 300µl homogenisation buffer(25mM HEPES pH 7.5; 5mM MgCL2; 1mM EGTA;

1mM Pefabloc SC; Protease-Inhibitor-cocktail (P8340, 1/100)) using the independent plastic pestle. The supernatant was collected and the protein-content was measured by using the BioRad Dc- Protein Assay according to the manufacturer's instructions. Each sample (100µL) was used with a final concentration of 0,5 µg/ml in homogenisation buffer. The assay was performed in duplicates for each biological replicate. The activity-measurement of effector caspases was measured by the CaspaseGLO 3/7 Kit from Promega Corp. (Madison, WI) as per the manufacturer's instruction usingwhite microwell-plates (Thermo Fisher scientific/Nunc,Roskilde, DK). One unit of active caspase(a recombinant mouse active caspase-3 from BioVision (Mountain View, CA)) was usedas positive control.The readout was measured using a LUMIstar Optima with the software Lumistar galaxy 4.30-0 from BMG Labtech (Offenburg, D) (Brodsky *et al.*, 2004; Das *et al.*, 2011). This experiment was performed and analysed by Hannes Temmel from the group of Univ. Prof. Dr. Gerald Hoefler, Institute of Pathology, at Medical University of Graz.

**26S proteasome activity assay**

The ATP-depended 26S proteasome-activity from the muscle was measured. The m.gast of MCK(m)-hLPL and the control mice were homogenized in 400µl homogenisation buffer (20mM Tris-HCl pH7.2; 0.1mM EDTA; 1mM 2-mercaptoethanol; 1mM DTT; 5mM ATP; 20% Glycerol (w/v); 0,04 (v/v) Triton X-100)usingthe MagNA-Lyser (Roche Diagnostics, Hoffmann-La Roche Ltd. Basel, CH). The protein content of the cell lysate was measured after protein precipitation using the BioRad Dc- Protein Assay. An aliquot of the cell lysate containing 40µg of protein was dissolved with the incubation-buffer (100mM Tris-HCl pH 7.4; 50mM HEPES pH 8.0; 5mM EGTA).The fluorogenic synthetic peptide (N-Succinyl-Leu-Leu-Val-Tyr-7-Amido -4-Methylcoumarin) was added at a final concentration of 0,167µg/µl. After 60 min of incubation at 37°C, the duplicates of each biological replicates were analysed for fluorescence at 355nm excitation and 460nm emission by conventional fluorometer (Brodsky *et al.*, 2004; Reinheckel *et al.*, 1998). This experiment was performed and analysed by Hannes Temmel from the group of Univ. Prof. Dr. Gerald Hoefler, Institute of Pathology at Medical University of Graz.

## *C2C12 cell culture*

Myoblast cell lines are useful for studies on skeletal muscle (SM) metabolism, and it has been demonstrated that the mouse C2C12 cell line develops biochemical and morphological properties as well as characteristics of SM (Gauthier-Rouviere *et al.*, 1996; McMahon *et al.*, 1994). The mouse C2C12 myoblasts were stably transduced with a retroviral vector encoding the full-length human LPL (hLPL) cDNA called LPL-OV cells. Control cells were transduced with a vector encoding b-galactosidase called C2-GEO cells. The LPL-OV C2C12 and the control C2-GEO cells were a generous gift from Dr.Eckel's research group, University of Colorado, Health Sciences Center (Poirier *et al.*, 2000). The C2C12 cells were cultured at standard cell culture conditions (37°C; 5% CO2) in growth medium (GM) consisting of RPMI 1640 high glucose medium, 10% FBS (foetal bovine serum) and 1x P/S (penicillin/streptomycin cocktail, PAA Laboratories GmbH,Pasching, A). When the C2C12 cells were grown at pre-confluence, the cellswere trypsinized and transferred to new cell culture plates before reaching100% confluence(Yaffe *et al.*, 1977). Cell counts were determined using a CASY TTC cell counter (Innovates AG, Bielefeld, D).

## *Estimation of C2C12 cell fusion index*

The LPL-OV C2C12 and the control C2-GEO cells were grown at 80 - 90% confluence. Myogenic differentiation was induced with differentiation media (2% Donor Horse Serum (HS); 1x P/S) (Soulez *et al.*, 1996). Every 2nd day the differentiation media was renewed. The progression of differentiation was observed by checking the myotube using an inverted microscope. At day six, the myotubes from LPL-OV and control C2C12cells were used for the studies (Blau *et al.*, 1985; Yaffe *et al.*, 1977). Myotubes were fixed with 2% formaldehyde in PBS and permeabilized with 0,1% Triton-X100 in PBS. For immunofluorescent staining of myotubes, the myotubes were incubated with the mouse monoclonal anti-MyHC (conc1:100 in PBS).A TRITC-conjugated goat anti-mouse-Alexa488antibody (conc1:500 in PBS) was used as secondary antibody. During the final 15 minutes of incubation with the secondary antibody a DAPI staining (conc1:1000) was added. Fluorescence signal was detected by 40x objective in the fluorescent microscope. Myogenic index in percentage was calculated from the below

mentioned equation from the myogenic staining of LPL-OV and control C2C12myotubes.

$$\text{Myogenic Index in percentage} = \frac{\text{Total number of nucleus - Number of nucleus in the myogenic tubes}}{\text{Total number of nucleus}} \times 100$$

## *Analysis of LPL activity of cells*

The LPL from the LPL-OV and control C2C12cells was isolated by an incubation with 2U/ml Heparin (37°C) (EBEWE-Pharma, Unterach am Attersee, Austria) in 1ml pre-warmed DMEM high glucose with L-glutamine containing 2% BSA (BSA Fraction 5,essentially FFA-free, Sigma-Aldrich, St. Louis, MO) for 1 hour at 37°C under constant gentle rocking. The supernatant(S/N) was collected to determine the LPL activity. The Protein content of remaining cells lysate was estimated using the Bio Rad Dc Protein assay according to the manufacturer's instruction. The LPL activity assay was performed as described by(Nilsson-Ehle, 1974). The measurement was performed using scintillation cocktail (Opti-Phase SuperMix, PerkinElmer Life and Analytical Sciences, Inc. (Waltham, MA)) anda β-counter (Beckman Coulter Inc. (Fullerton, CA) type LS 6500 Multi-Purpose Scintillation Counter)(Nilsson-Ehle, 1974).This experiment was performed and analysed by Hannes Temmel from the group of Univ. Prof. Dr. Gerald Hoefler, Institute of Pathology at Medical University of Graz.

## *Staining of lipids*

On day 6 of differentiation myotubes within LPL-OV and control C2C12cultureswere analysed for lipid by a staining with saturated Nile Red in acetone solution (diluted 1:10). Similarly, the lipid accumulation was also checked with a second method using BODIPY 493/503 dye (Molecular Probes, Eugene, OR, USA) in GM for 3h at 37°C CO2 incubator for 3 hours(Greenspan *et al.*, 1985; Zhang *et al.*, 2010).Lipid accumulation as measured bynile red staining (this experiment was performed and analysed by Hannes Temmel from the group of Univ. Prof. Dr. Gerald Hoefler, Institute of Pathology at Medical University of Graz).The BODIPY signal was detected using a 40x objective of a fluorescent microscope. The Nile Red and BODIPY images were examined using a

microscope from Nikon (Eclipse TE 2000U; x-cite 120 FluoresExfo of the NIKON Corporation Tokyo, Japan).

## *qRT PCR from the RNA from C2C12 cells*

Total RNAs were extracted from LPL-OV and control C2C12cells at day zero and day 6 (differentiated myotubes) with the TRIZOL. From each sample, one microgram RNA was used for reverse transcription using "High Capacity cDNA Reverse Transcription Kit (Applied Biosystems) according to the manufacturer's instructions. The cDNA-samples (5µl of 1:20 dilutions) were used in triplicates for qPCR to relatively quantify mRNA expression of the genes using the primers mentioned in the table below. The primers were designed as described previously.

**qPCR Primers**

| | | | |
|---|---|---|---|
| Murine myogenin | mMyogenin | Sense | 5'-CAGCTCCCTCAACCAGGAG-3' |
| | mMyogenin | antisense | 5'-TGGGAGTTGCATTCACTGG-3') |
| Human LPL | hLPL | Sense | 5'-GTCACGGGCTCAGGAGCATT-3' |
| | | antisense | 5'-ACAGGATGTGGCCCGGTTTA-3' |
| 18s Ribosome | 18s | Sense | 5'-GTAACCCGTTGAACCCCATT-3' |
| | | antisense | 5'-CCATCCAATCGGTGTGCG-3' |

## *Biochemical determination of FFA and TG*

The LPL-OV and control myotubes at the 6$^{th}$ day of differentiation were starved for serum for 6 hours. The lipid samples were isolated by Hexane isoproponal method (Hara *et al.*, 1978). The FFA and TG were measured from the chloroform phase (TG measurement was performed and analysed by Hannes Temmel from the group of Univ. Prof. Dr. Gerald Hoefler, Institute of Pathology at Medical University of Graz.). The samples were brought to dryness under nitrogen gas. The resulting lipid pellets were solubilised in 2% Triton X-100 by sonication. The FFAs were quantified by using the NEFA-HR(2) kit from Wako Chemicals GmbH and TG was measured with the Triglyceride FS kit from DiaSys Diagnostic Systems (Holzheim GER) according to the manufacturer's instructions (Hara *et al* 1978).

## *Developing the h-LPL regulated expression cloning.*

The hLPL mini gene with the gene of glycosylphosphatidylinositol (GPI) anchored protein(LPL-GPI), which was a generous gift from Goldberg IJ Dept. of Medicine, Columbia University, Newyork, USA., was used to develop the cloning plasmid to create the controlled expression (by Tet-on expression system) of hLPL in the C2C12 cells. hLPL expression is induced by doxycycline (dox).The LPL-GPI was isolated by restriction enzyme digestion using Cla1 and EcoRV (fermentas Fisher Scientific Austria GmbH) as per the protocol supplied by the company. The LPL-GPI gene was cloned into the Retro-X$^{TM}$ Tet-on Advanced Inducible Expression System (Clontecheubio Wien Austria). The right orientation of the insert to the plasmid was analyzed by a Hind III restriction enzyme digest. The cloning of a LPL-GPI gene and developing the stable inducible expression of hLPL in C2C12 cells was done according to the Tet-on Advanced Inducible Expression System's manufacturer instruction.

## *Analysis of dox inducible hLPL expression in C2C12 cells*

Arround 30 clones of dox induced expression of hLPL in the C2C12were created and analysed for mRNA expression of hLPL. The best clones of C2C12 cells were induced with 0.5µg of doxycycline, and analysed for the myogenic tube formation.

## *Animal care and use*

The C57BL/6 mice were maintained on a regular light-dark cycle, (12 h light, 12 h dark) and kept on a standard laboratory chow diet (4.5% w/w fat).The mice were bred to develop the minimum number mice which were required to study the role of ATGL in tumor metabolism. Mice used for these studies were between 9-10 weeks old. All experiments were performed according to the animal protocol approved by the Austrian government (BMWF-66.010/0110-II/3b/2010).

## *Atgl-ko and Wt B-cells*

The suspension tumor B-cells were generated in the lab from Univ. Prof. Dr. Veronika Sexl (Institute of Biomolecular Medicine and Pharmacology, Medical University of Vienna). The morphology of these suspension cells is round shaped, and they were developed from the bone marrow cells from ATGL-ko mice and wild type mice. The B-cells were transduced by p185bcr-abl and GFP with the viral

supernatant of Φ-NX (Phoenix) cells. The Atgl-ko and wt cells were propagated in RPMI media with L-Glutamine, FBS (10%),P/S (1%) and 0.1mM Beta mercaptoethanol. For sub-culturing cells were centrifuged at 900 RPM for 4 minutes at room temperature, dissolved in fresh media and transferred to a new cell culture dish. The cells were maintained in a CO2 cell culture incubator at 37°Cuntil the cells reached sufficient cell number. The Atgl-ko and Wt cells (150,000 cells) were used for injection per mouse.

### *LLC-Atgl-ko and LLC-wt cells*

The LLC cells were cultured in DMEM media containing L-Glutamine, 10 % FBS, and 1% P/S at 37°Celcius in a CO2 incubator. The ATGL was inhibited in the LLC LLC-ATGL-kd (knock down). The stable cells of LLC-ATGL-kd were developed by inhibiting the ATGL with the shRNA, and the control LLC-wt cells were developed with scrambled shRNA by Dr.Suman Kumar Das from the group of Univ. Prof. Dr. Gerald Hoefler, Institute of Pathology at Medical University of Graz.For propagation LLC-ATGL-kd and LLC-wt cells were trypsinized and centrifuged at 900 RPM for 4 minutes at room temperature. The cell pellet was dissolved in fresh media, and the cells were transferred in to anew cell culture dish in culture condition at 37°Celcius in CO2 incubator. The LLC-ATGL-kd and LLC-wt cells were continuously propagated until the cells reached sufficient cell number The LLC-ATGL-kd and LLC-wt cells (2,5 million cells) were used for injection per mouse.

### *In vitro cell culture proliferation and ATGL expression*

Six clones of B-cells with Atgl-ko and three clones Wt B-cells were analyzed for the proliferation for 4days by using CASY count according to the manual of CASY count instrument. Three clones of Atgl-ko and Wt B-cells were analyzed for the mRNA expression of ATGL.

### *Tumor proliferation in wt mice*

To study the proliferation of induced tumors in mice, the Atgl-ko and Wt B-cells were injected subcutaneously in the *dorsum* just below the neck of the mice for all the studies. All the mice were sacrificed in the afternoon to harvest the tumor.

### *In vivo tumor growth using various cell numbers and various periods of time*

In order to define the suitable duration and the appropriate cell number for tumor induction in mice, the mice were divided in to three groups. The first groups of mice were injected with 100,000 cells of Atgl-ko and Wt B-cells, respectively. The tumor was isolated after 16 days and tumor weight was measured. The second group of mice were injected with 0,5 million cells of Atgl-ko and WtB-cells. The tumor was isolated after 13 days, and tumor weight was measured.The last groups of mice were injected with 1million cells of Atgl-ko and WtB-cells. The tumor was isolated after 16 days, and tumor weight was measured.

### *In vivo tumor growth studies on LLC-Atgl-ko and LLC-wt cells*

The LLC-ATGL-ko and LLC-wt cells were used as another *in vivo* tumor model to analyze the role ATGL. The cells were cultured in the CO2 incubator with the culture conditions mentioned earlier. The C57BL/6 mice were grouped into two sets. One group of mice were injected subcutaneously in the *dorsum* just below the neck with 2.5 million cells of LLC-ATGL-ko. The second group of mice were injected with same amount of LLC-wt cells. The mice were carefully monitored for visible tumor growth. After 14 days the mice from both groups were anesthetized with isoflurane, and sacrificed by cervical dislocation. The isolated tumor samples were weighted, and stored in liquid nitrogen.

### *In vivo tumor growth studies on various genotypes of mice*

The number of injected cells of 150,000 Atgl-ko and Wt B-cells was constantly maintained for all the experiments used to study the tumor growth of various genotypes of mice.

The Atgl-ko and Wt cells were injected into the mice, and the mice were carefully observed for visible tumor growth. The tumor was isolated 14 days after tumor cell injection, and analyzed for the tumor weight, and stored in the liquid nitrogen for further analysis. In order to study whether the tumor growth is related to the gender, the immune system, or PPAR activation, Atgl-ko and Wt B-cells were injected according to the following conditions:(i)Male C57BL/6 mice, (ii)Female

C57BL/6 mice, (iii)Atgl-ko mice, (iv)RAG2 mice, (v)RAG2 gamma mice, Finally, (vi) Normal mice (C57BL/6) fed with fenofibrate supplemented food.

### *Genes expression analysis of tumor by Affimetrix chip*

Atgl-ko and Wt B-cells were injected into Wt mice. In order to maintain the same size of tumor in both groups of mice, the mice were carefully observed for tumor growth. Mice were sacrificed after a different period of time to allow for approximately similar tumor weight in both the groups. The RNA was extracted, and sent to the ZMF core facility to analyze gene expression using an affymetrix chip (GeneChip Mouse Gene 1.0 ST Array, Affymetrix,High Wycombe, UK). mRNA expression was also analyzed by qRT-PCR to verify the result of selected genes from the Affymetrix chip.

## Statistics

Results are expressed as means ± s.e.m. Statistical significance was tested by unpaired t-test with Welch´s correction. The statistical analyses were performed using Graphpad Prism version 5. The $P< 0.05$ was considered as significant. The number of stars indicate the value of significance as follows: $p$= *** < 0,001,$p$= ** < 0,01, and $p$= * < 0,05. The standard deviation is indicated by + error bar.

# Results

## *MCK-driven hLPL expression in the mice caused skeletal muscle loss and impaired physical stamina*

This result section is partially reused from the publication (Tamilarasan *et al.*, 2012)with modifications. The materials are reproduced with the permission of Nature Publishing Group.

The previous studies on the skeletal muscle demonstrated that the MCK-driven hLPL expression caused eight-fold increased LPL activity in the skeletal muscle. The increased LPL activity leads to the development of histological as well as pathological changes in the adult MCK(m)-hLPL mice (Hoefler *et al.*, 1997; Levak-Frank *et al.*, 1995; Sattler *et al.*, 1996; Voshol *et al.*, 2001). MCK(m)-hLPL mice might be physically impaired.C57Bl/6J × CB Wt mice and isogenic MCK(m)-hLPL mice were used in these studies. In order to analyse the physical stamina of the MCK(m)-hLPL mice, treadmill experiments were performed. Results from the treadmill experiment showed that MCK(m)-hLPL mice with the age of 4-6 months had more impaired physical stamina than the control isogenic wild-type (Wt) mice (Figure 8a).To understand the effect of impaired physical stamina related to hLPL over expression on skeletal muscle, the three different types of the skeletal muscles which are m.gast, m.quad and m.sol were isolated for analysis. The transgenic hLPL mRNA expression was measured from those muscles by qPCR. The results from the qPCRs confirmed the strong expression of hLPL mRNA in m.gast (3.81±0.39-fold lower signal than 18s rRNA), m.quad (3.7±0.46-fold lower signal than 18s rRNA) and m.sol (10.33±3.5-fold lower signal than 18s rRNA) of MCK(m)-hLPL mice compared to control (data not shown). However,the hLPL expression in them.solwas approximately three-fold less compared with m.gast and m.quad of MCK(m)-hLPL mice. Moreover, no hLPL (mRNA) was detectable in Wt mice(n=5). Therefore, the expression of hLPL in muscles from MCK(m)-hLPL mice is given as the relative to the expression of the corresponding reference gene. The skeletal muscle weight was significantly decreased in m.gastand m.quad from MCK(m)-hLPL mice compared to Wt mice (m.gast 2.51±0.28 versus 4.70±0.39 mg/g and m.quad 2.29±0.9 versus 5.59±0.77 mg/g, ***P<0.0001, Figure 8c and 8b). However, there was, no significant difference in the muscle

weight between the m.sol from MCK(m)-hLPL mice and Wt mice (Figure 8d).The difference in muscle weight was macroscopically obvious by the hypotrophic appearance of m.gast and m.quad from MCK(m)-hLPL mice, illustrating the differences between the two genotypes (Figure 8e).The deficiencies of the physical performance of MCK-hLPL mice caused by the muscle mass loss could correspond to sarcomeric aberrations. In fact, electron microscopic (EM) analysis showed aberrations of the sarcomers of MCK-hLPL skeletal muscle. Furthermore, the EM analysis revealed the focal disruption of sarcomere units with ultra-structural irregularities in the m.gast of MCK(m)-hLPL mice compared to the m.gast from control Wt mice(Figure 8f).However, the m.sol of MCK(m)-hLPL mice did not show the focal disruption of sarcomere units (Figure 8g).

**FIGURE 8**

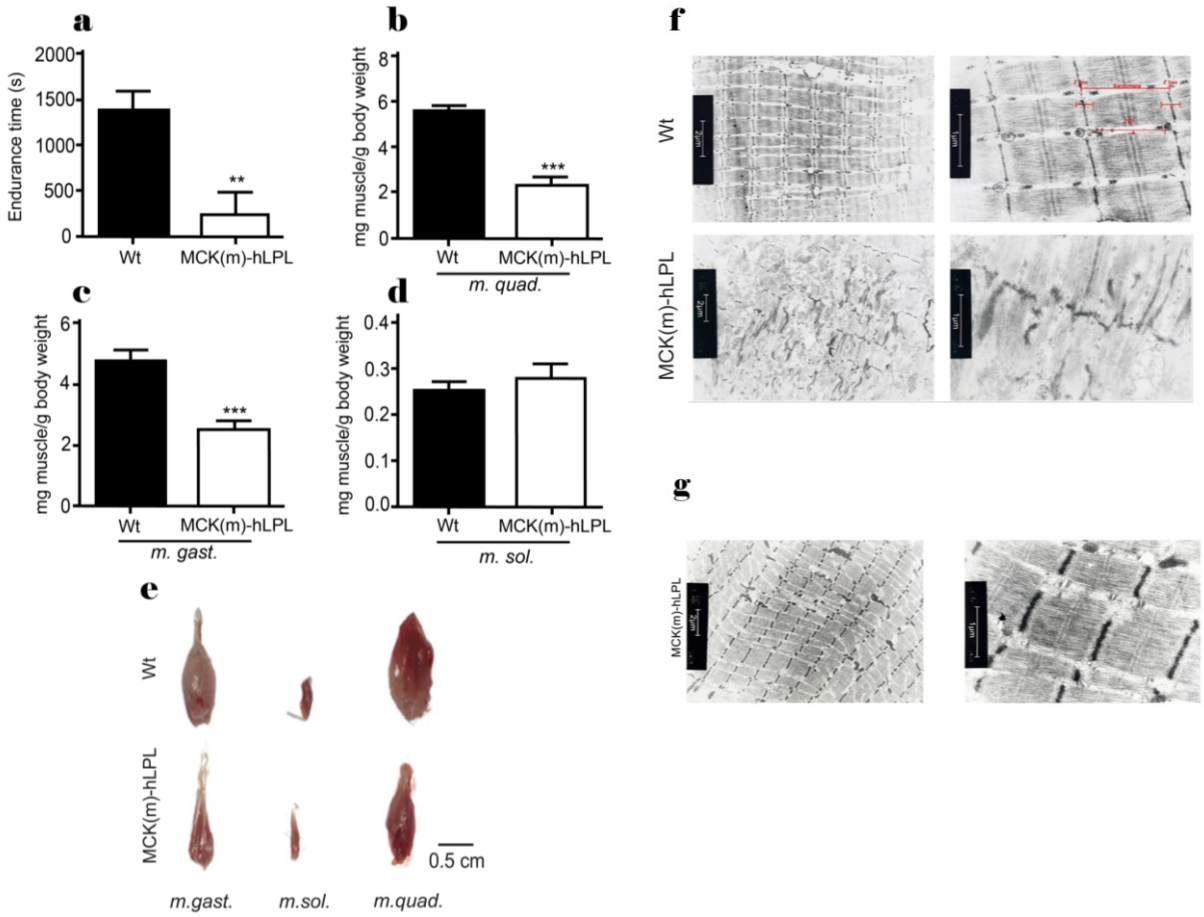


**Figure 8 a** The physical endurance of MCK(m)-hLPL and control isogenic mice (n=3; age=4 month), was estimated by the treadmill approach (V=0.25 m/s). Whenever the mice reached to the end of the treadmill lane, a mild electric stimulus was delivered at the rear end of the treadmill. The time that elapsed until 10 stimuli occurred is presented as mean value ±SD of the endurance time. The endurance time ofMCK(m)-hLPL mice was significantly lower than that of control Wt mice (226±252 sec. versus 1379±209 sec., **P<0.005). **b** Mice(n=3; age=6 month) were sacrificed and the m.quad weight was measured from MCK(m)-hLPL and control mice. The weight of the m.quad from MCK(m)-hLPL mice was significantly less than the one from control mice (2.29± 0.9 mg/g vs 5.59± 0.77 mg/g, p= 0.0001). **c** Mice (n=5; age=6 month) were sacrificed and the m.gast weight was measured from MCK(m)-hLPL and control mice. The weight of m.gast from MCK(m)-hLPL mice was significantly less than the m.gast from control mice (2.51± 0.28 mg/g vs 4.70± 0.39 mg/g, p= 0.0001). **d** Mice (n=5; age=6 month) were sacrificed and the m.sol weight was measured from MCK(m)-hLPL and control mice. The weight of m.sol from MCK(m)-hLPLwas not significant different compared to the control mice (0.28 ±0.02 mg/g vs 0.19± 0.025 mg/g, p=0.008). **e** Representative images of m.gast, m.sol, and m.quad preparations indicated the anatomically correct preparation of the muscle sample. The hypotrophic appearance of the m.gast and m. quad

from MCK(m)-hLPL mice (lower panal), illustrates the visual difference between the muscles from MCK(m)-hLPL and Wt mice The skeletal muscle tissue was isolated and photographed by Suman Dasfrom the group of Univ. Prof. Dr. Gerald Hoefler, Institute of Pathology at Medical University of Graz. **f** m.gast tissue samples from the MCK(m)-hLPL and control mice (n=3, age=6 month) were analyzed by EM. The full sacromere unit without irregularities in the myofibrillar structure of the m.gast from Wt mice is shown in the upper panel. The normal muscle structure is characterized by clearly defined Z-lines, H-band, A-bands and I-bands (upper right panel).Irregularities of sacromeres with hardly defined myofibrillar structures from the m.gast from MCK(m)-hLPL mice are shown in the lower panel. **g** The m.sol. tissue samples from the MCK(m)-hLPL and control mice (n=3, age=6 month ) were analyzed by EM. The image indicates the full sacromere unit without irregularities of myofibrillar structures of the m.sol.Thisexperiment was performed and analysed by Hannes Temmel from the group of Univ. Prof. Dr. Gerald Hoefler, Institute of Pathology at Medical University of Graz.

## *Muscles of MCK(m)-hLPL mice contained elevated lipids and increased protein degradation leads to lipoapoptosis*

This result section is partially reused from Tamilarasan *et al* with modifications. The materials are reproduced with the permission of Nature Publishing Group.

**Increase in the lipid uptake was noticed in the MCK(m)-hLPL mice.**

The increased hLPL mRNA expression of the skeletal muscle of MCK(m)-hLPL could lead to increase the lipids in the skeletal muscle which might be one of reasons for its poor physical stamina. The FFA and the TG from the skeletal muscle of MCK(m)-hLPL were increased compared to the control. Analysis of the muscle lipid content from the anatomically prepared entire m.gast muscles of 12 h fasted MCK(m)-hLPL mice showed >3-fold elevated FFA levels(Figure 9a,***P<0.0001) and>4-fold increased TG levels (Figure 9b, **P<0.005) compared to Wt mice. However the FFA and TG levels of the m.sol were elevated to a lesser degree in MCK(m)-hLPL compared toWt mice (Figure 9c,Figure 9d).

**FIGURE 9**

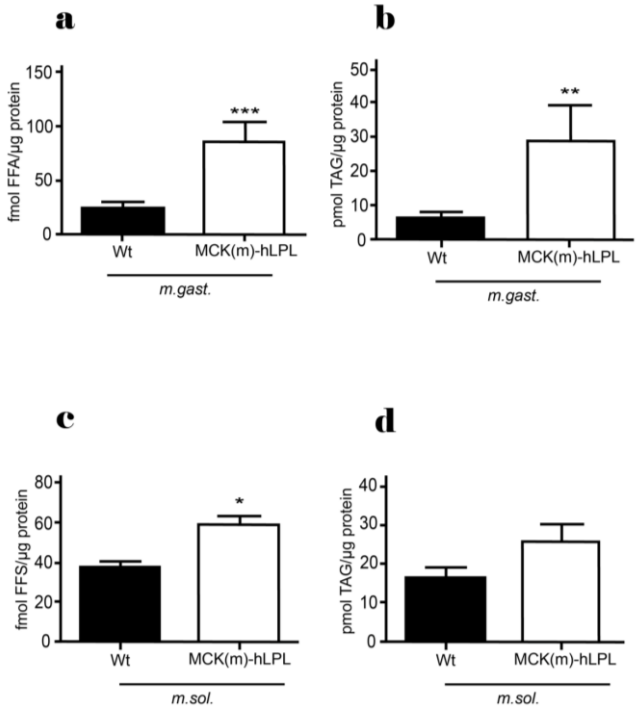


**Figure 9 a** The FFA estimation of m.gast from 12 h fasted MCK(m)-hLPL and Wt mice (n=6; age=6 month) was measured biochemically as mentioned in the materials and methods. The FFA levels were significantly increased in m.gast of MCK(m)-hLPL compared with Wt mice (85.84±17.39 versus 25.0±4.3 fmol/µg, ***P<0.0001). **b** The TG estimation of m.gast from 12 h fasted MCK(m)-hLPL and Wt mice (n=6; age=6 month) was measured biochemically as mentioned in the materials and methods. The TG levels were significantly increased in m.gast of MCK(m)-hLPL compared with Wt mice (28.71±10.49 versus 6.48±1.62 pmol/µg ,**P<0.005). **c** The FFA analysis of m.sol from 12 h fasted MCK(m)-hLPL and Wt mice (n=6; age=6 month) showed significantly increased FFA levels in m.sol of MCK(m)-hLPL compared with Wt mice (58.79±4.34 versus 39.06±2.19 fmol/µg, *P<0.05). **d** The TG estimation of m.sol from 12 h fasted MCK(m)-hLPL and wt mice (n=6; age=6 month) revealed no significant difference in m.sol.of MCK(m)-hLPL compared with Wt mice (25.82±4.47 versus 16.88±2.65 fmol/µg).

**Increase in the apoptosis was observed in the MCK(m)-hLPL mice.**

Increased lipid levels in the cells could lead to increased apoptosis. Indeed, increased apoptosis was observed in m.gast of MCK(m)-hLPL by many methods: tunel staining, the 26S ATP dependent proteasomal activity, IHC of caspase3, and Caspase3/7 enzymatic activity assay. In summary, tunel staining of the tissues showed a significantly higher percentage of apoptotic nuclei in m.gast of MCK(m)-hLPL mice compared with Wt (2.83±0.24% versus 0.84±0.37%, **P<0.005, Figure 10a and 10b). In addition, positive IHC of active caspase3 was detected in the m.gast (Figure 10c). Further studies indicated that the 26S proteasome-dependent proteolysis was significantly increased on average by 79.8% (*P<0.05) in the MCK(m)-hLPL mice compared with Wt, (Figure 10d) and also increased caspase 3/7 activity was noticed in muscles of MCK(m)-hLPL compared to Wt mice (343.3 ± 27.07 RLU / µg versus 248.4 ± 18.13 RLU / µg, Figure 10e).However, the elevated FFA, TG, and apoptosis effects might be just a consequence of fiber-type differences between LPL transgenic and Wt mice, but the subsequent fiber-type analysis indicated that there is no difference in the fiber type comparing the hLPL over expressing and the control muscle. However, the percentages of the fast twitch (type II) fibers were much higher in m.gast and m.quad when compared with m.sol. Although, there was no differences in the percentage of type I and type II fibers between the MCK(m)-hLPL and Wt mice within each muscle group (m.gast, m.sol and m.quad indicated in Figure 10f and Figure 10g).

## FIGURE 10

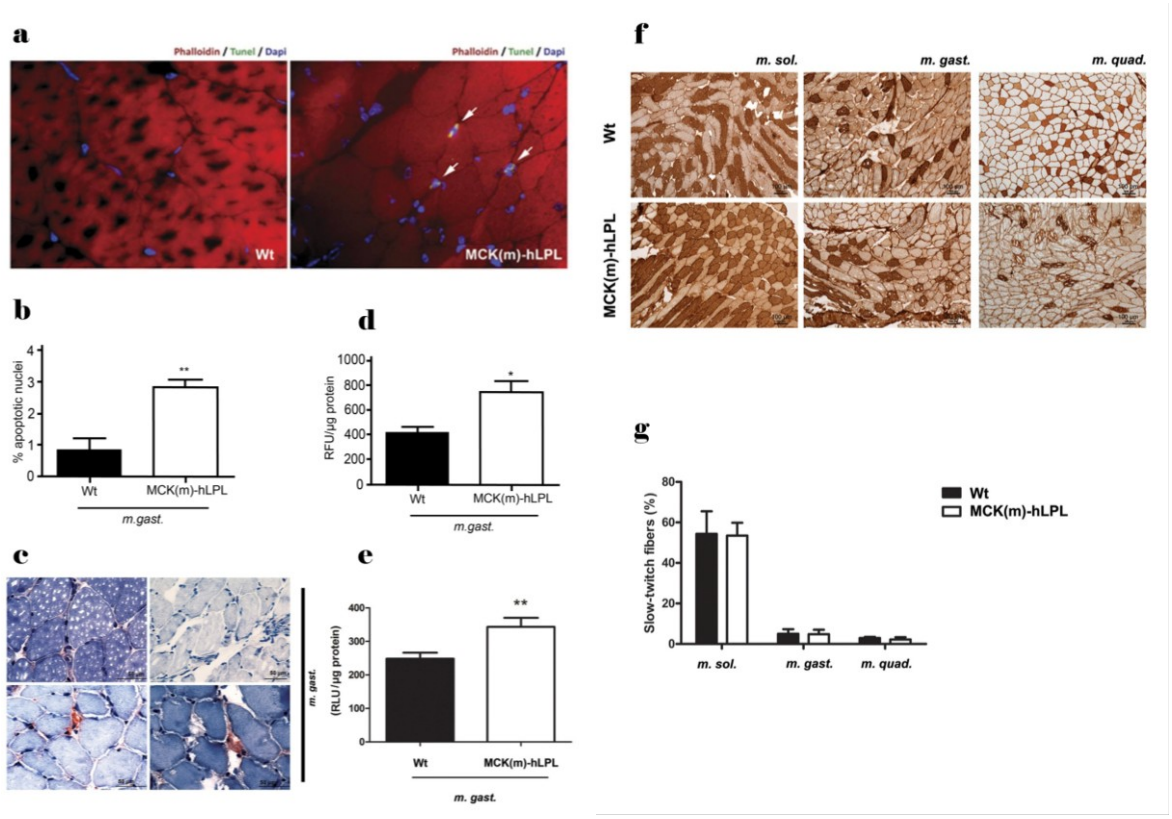


**Figure 10 a** The TdT-mediated dUTP nick end label (TUNEL) staining of transverse sections of m.gast from the MCK(m)-hLPL and Wt mice was analysed for apoptotic cells. TUNEL-positive apoptotic nucleiare stained in bright green. Representative section of the tunel staining is shown, and the positive nuclei are highlighted with arrows. Phalloidin and DAPI were used as counter stain for actin filaments and the nuclei. The staining was performed by Silvia Schauer from the group of Univ. Prof. Dr. Gerald Hoefler, Institute of Pathology at Medical University of Graz. **b** Total number of 10 fields of view (× 100 magnification) encompassing >300 nuclei were counted from each tissue section (n=4) from the TUNEL staining. MCK(m)-hLPL m.gast showed a significantly higher percentage of apoptotic nuclei compared with the m.gast of Wt mice(2.83±0.24% versus 0.84±0.37%, **P<0.005).This data was analysed by pathologist Dr. Wael AlZoughbi from the group of Univ. Prof. Dr. Gerald Hoefler, Institute of Pathology at Medical University of Graz. **c** IHC using antibodies detecting active caspase3 was performed on paraffin embedded m.gast sections from MCK(m)-hLPL and Wt mice (n=6). Distinctively stained cells were only observed in MCK(m)-hLPL m.gast (representative images in lower panels) but not in Wt muscles (upper left panel) or in MCK(m)-hLPL muscles stained without primary antibody (negative control, upper right panel). Size bars: 50 µm. This exprement was performed by Silvia Schauer from the group of Univ. Prof. Dr. Gerald Hoefler, Institute of Pathology at Medical University of Graz. **d** The 26S ATP-depended proteasomal enzymatic activity was measured biochemically from the extracts of transversal cross sections of m.gast of MCK(m)-hLPL and Wt mice. The ATP enzymatic activity was presented as relative fluorescence units (RFU)/µg protein that is significantly higher 26S-protesome activity was

observed in m.gast of MCK(m)-hLPL compared with Wt mice (739.5±91.5 versus 411.4±45.1 RFU/µg protein, *P<0.05; n=3). This experiment was performed and analysed by Hannes Temmel from the group of Univ. Prof. Dr. Gerald Hoefler, Institute of Pathology at Medical University of Graz. **e** TheCaspase 3/7 enzymatic activity was biochemically measured in m.gast from MCK(m)-hLPL and Wt mice (n=4). The enzymatic activity is presented as relative luminescence units (RLU)/µg protein that is significantly increased caspase 3/7 activities were observed in muscles of MCK(m)-hLPL compared to Wt mice (343.3 ± 27.07 RLU/µg versus 248.4 ± 18.13 RLU/µg).This experiment was performed and analysed by Hannes Temmel from the group of Univ. Prof. Dr. Gerald Hoefler Institute of Pathology at Medical University of Graz. **f** The representative images of the fiber type analysis was performed usingIHCfor slow (type I) and fast (type II; data not shown) myosin from whole transverse sections from m.sol, m.gast and m.quad. The staining was performed by Silvia Schauer from the group of Univ. Prof. Dr. Gerald Hoefler, Institute of Pathology at Medical University of Graz. **g** The relative amount of type I myosin was calculated from the representative images of type I staining (by IHC). 600 - 1500 (m.gast *and .quad*) or 50-150 (*m.sol*) fibers of each muscle were counted. The relative amount of type I myosin positive fibers of total fibers is given in % for each muscle. Mean values± SEM: *m.sol*: 54.34 ± 5.566 versus 53.49 ±3.174, n=4; m.gast*:* 5.059 ± 0.9021, n=6 versus 4.856 ± 1.078, n=4; *m.quad*: 2.975 ± 0.3730, n=3 vs. 2.203 ± 0.8142, n=3). There is no statistically significant difference between the two genotypes. These data was analysed by pathologist Dr. Wael Alzoughbi from the group of Univ. Prof. Dr. Gerald Hoefler, Institute of Pathology at Medical University of Graz.

## *Over expression of hLPL in muscle cells reduced the regenerative and myogenic capacity*

This result section is partially reused from Tamilarasan *et al* with modifications. The materials are reproduced with the permission of Nature Publishing Group.

**Skeletal muscle regeneration was impaired in the MCK(m)-hLPL mice**

In general, the previous studies indicated that skeletal muscle satellite cells were activated during the muscle injury or disease condition. Furthermore, the skeletal muscle satellite cells could develop muscle myoblasts. Indeed, during this process they undergo proliferation and eventually differentiation to form new muscle fibers which allows for proper muscle regeneration (Charge *et al.*, 2004; Mauro, 1961). The protein degradation and apoptosis in skeletal muscle might play an important role in altered muscle regeneration in the MCK(m)-hLPL mice because of its lipotoxic effects. The muscle regeneration can be studied by the analysis of the recovery of cobra toxin (CTX) induced damage in the m.gast of mice. The m.gast from MCK(m)-hLPL showed delay in muscle regeneration compared to control. Regeneration in terms of the average cross section area (XSA) of muscle fibers was significantly decreased in the MCK(m)-hLPL CTX versus the sham group after 10 days of regeneration (64.5±20.1%, *P<0.05), whereas Wt muscle fibers had already almost reached their normal XSA (98.1±18.3%) of muscle regeneration (Figure 11a, Figure 11b).The m.edl and m.sol of CTX-injected mice or in sham-injected muscles there was no tissue damage detected (data not shown). The staining was performed by Silvia Schauer and the data was analysed by pathologist Dr. Wael Alzoughbiboth of them were from the group of Univ. Prof. Dr. Gerald Hoefler, Institute of Pathology at Medical University of Graz.

**FIGURE 11**

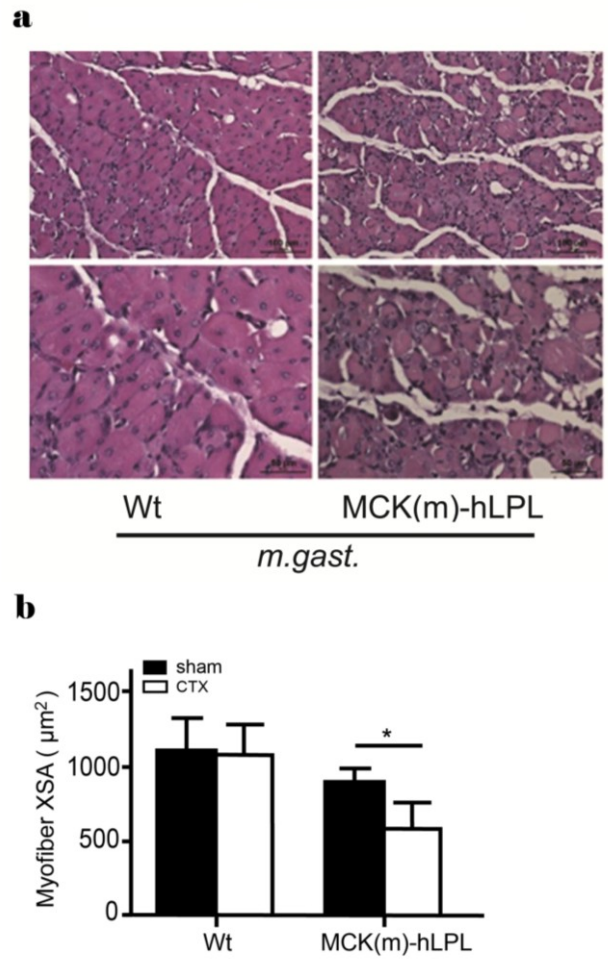


**Figure 11 a** The H&E staining of m.gast from CTX injected MCK(m)-hLPL and Wt mice. Representative sections demonstrate that CTX injury was confined to m.gast. Tissue sections from m.gast showed regenerating fibers that are characterized by centralized nuclei, whereas muscle fibers of m.edlor m.sol did not show an injury or regeneration (data not shown). **b** Images of myofibers were captured from the H&E-stained tissue section indicated in the Figure 11a. Myofiber XSA of 100–260 myofibers within a fixed area (289 319 µm2) were measured. Measurements of myofibers in CTX-injected mice were performed in the regenerating areas as defined by centrally localized nuclei. It was shown that the average XSA of muscle fibers in MCK(m)-hLPL mice was significantly reduced 10 days after CTX versus sham-injected mice (64.5±20.1%, *P<0.05). No statistically significant difference was observed in Wt mice between CTX- and sham-injected mice (98.1±18.3%)The tissue staining was performed by Silvia Schauer and the data analysis by pathologist Dr. Wael Alzoughbi both of them were from the group of Univ. Prof. Dr. Gerald Hoefler, Institute of Pathology at Medical University of Graz.

### *In vitro cell culture of myotube differentiation of C2C12 cells*

In order to study the mechanism of the lipotoxic effects to the skeletal muscle regeneration, the continuous murine myoblast cell line C2C12 was used. Several studies indicated that cultured C2C12 cells can be differentiated into myotubes, and the myotube formation is as an excellent model system to study myogenesis (Charge *et al.*, 2004; McNally *et al.*, 2007).The proliferation analyzed for C2-GEO control and LPL-OV cells in 10% FBS proliferation medium, prior to induction of differentiation showed no difference (Figure 12a). At the same time the cell viability was estimated by using trypan blue exclusion assay in confluent C2-GEO control and LPL-OV cultures which also was found to be comparable between both phenotypes (Figure 12b). Further, the over expression of hLPL in the C2C12 cells caused altered differentiation potential compared to control cells (C2-GEO). The observed time course of differentiation of C2C12 cells after induction on day zero, day three and day six (d0, d3 and d6) is depicted in Figure 12c.

**FIGURE 12**

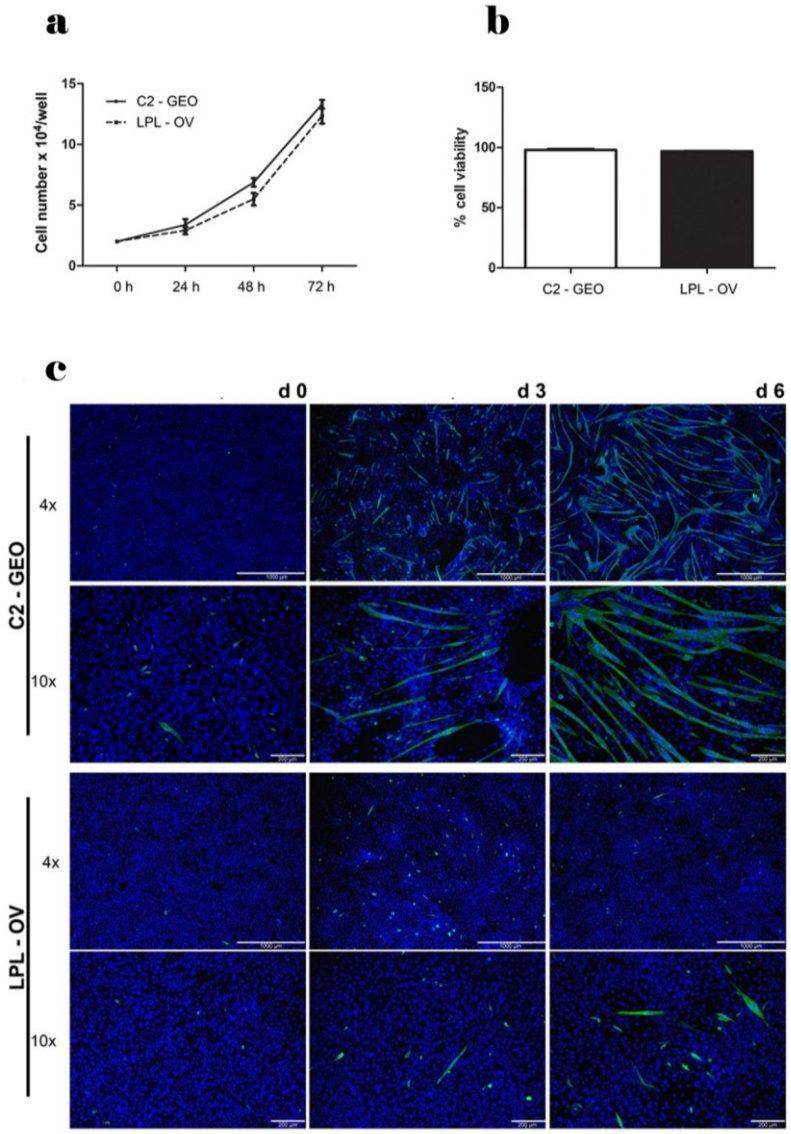


**Figure 12 a** Cell proliferation was determined for C2-GEO control and LPL-OV cells in 10% FBS proliferation medium, prior to induction of differentiation. There was no difference in the cell proliferation between the two phenotypes. **b** The cell viability was recorded using trypan blue exclusion assay in confluent C2-GEO control and LPL-OV cultures just before induction of differentiation in parallel cultures which were than used to determine fusion index. There was no difference in the cells were observed concerning cell viability MTT assay between the C2-GEO control and LPL-OV cells. **c** Time course images of C2C12 cell differentiation after induction of confluent cultures by 2% HS at day zero, day three and day six (d0, d3 and d6). The cells were fixed, and stained with anti-myosin heavy chain antibody (MyHC), followed by immunofluorescence detection to visualize myotubes (green channel) and nuclei (stained with DAPI; blue channel). There are two different magnifications (4x and 10x) of representative images showed which is indicating that the LPL-OV cells showed poor differentiation compared to control C2-GEO cells.

**The differentiation markers MyHC and MyoD were reduced in the C2C12 LPL- OV cells.**

The observation of altered myotubes formation in the LPL-OV cells might be due to a modified expression of MyHC and MyoD. Moreover, the expression of hLPL as well as the LPL activity was analyzed. The fusion index was calculated from the IHC image of the MyHC. Representative images are shown in Figure 13a.The observed result indicated a significantly decreased fusion index (**P<0.005, Figure 13b). In addition, the mRNA expression of MyoD as well as hLPL expression in C2C12 cells after 6 days of differentiation were significantly reduced (Figure 13c, Figure 13d). Moreover, the LPL activity was significantly increased in the LPL-OV, (Figure 13e).

## FIGURE 13

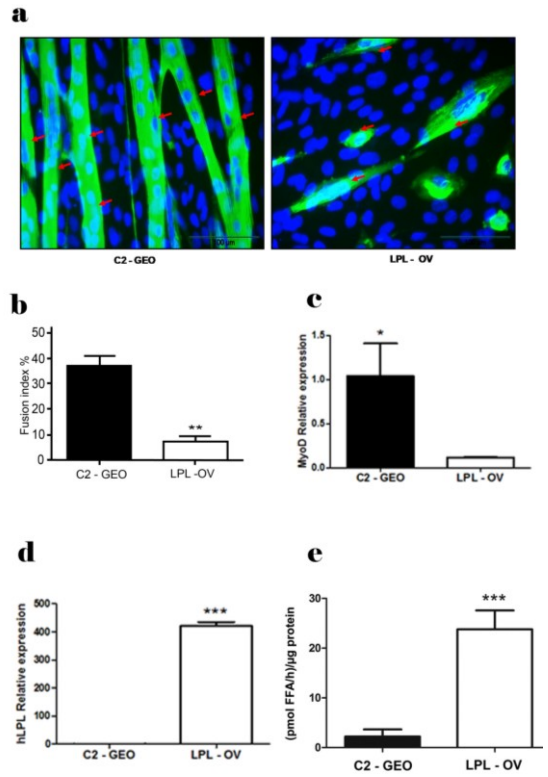


**Figure 13 a** LPL-OV as well as the control C2-GEO cells (n=3), were induced for differentiation into myotubes by medium containing 2% HS after reaching confluence. The cells were differentiated to myotubes at day six. The differentiated cells were fixed and treated with anti-MyHC antibody followed by immunofluorescence detection to visualize myotubes (green channel) and nuclei (stained with DAPI; blue channel). Representative images are shown. The myotubes are indicated by red arrows. **b** The fusion indices were calculated from the myotube immunostaining with anti-MyHC antibody. Five images of each cell culture were analysed. The fusion index represents mean values of nuclei in MyHC-positive stained areas versus total number of nuclei per image in percent ±SD. The fusion index of LPL-OV proved to be significantly lower than the control C2-GEO cells (7.44±2.07% versus 36.86±4.12%, **P<0.005). **c** The mRNA expression was analyzed for MyoD. The relative expression of MyoD was significantly reduced in the LPL-OV cells compared to control C2-GEO cells. The 18s ribosomal RNA was used for normalization. **d** Analysis of the hLPL mRNA expression showed that the relative expression of hLPL was significantly increased in LPL-OV cells compared to control C2-GEO cells. For normalization the 18s ribosomal RNA was used. **e** LPL activity was determined by estimating FFA release at day 6 of myogenically differentiated LPL-OV and C2-GEO cells (n=5). FFA released by hLPL is given in (pmol FFA/h)/µg protein ± SD. Significantly higher LPL activity was observed in LPL-OV cells compared to C2-GEO cells (23.79 ± 3.79 [pmol/µg]/h versus 2.21 ± 1.46 [pmol/µg]/h, P<0.0001).This experiment was performed and analysed by Hannes Temmel from the group of Univ. Prof. Dr. Gerald Hoefler, Institute of Pathology at Medical University of Graz.

**The lipid in the LPL-OV cells was increased compared to the control C2-GEO cells.**

This result section is partially reused from Tamilarasan *et al* with modifications. The materials are reproduced with the permission of Nature Publishing Group.

The increased expression of hLPL as well as the elevated LPL activity might increase the amount of lipids in the cells. The lipid staining with nile red as well as bodipy on the $6^{th}$ day of differentiation of LPL-OV cells and control C2-GEO cells indicated the presence of more lipids in LPL-OV cells. Representative images of lipid staining with nile red and bodipy are shown in Figure 14a and 14c, respectively. The arbitrary units of the lipid were calculated from the image of lipid staining indicating that both, the nile red as well as the bodipy staining showed significantly increased lipid accumulation in the LPL-OV cells compared to control C2-GEO cells (Figure 14b and Figure 14d). In addition, functional hLPL over expression, which caused increased lipid levels, was confirmed again by the biochemical analysis of intracellular FFA and TG in the LPL-OV cells. The observed results showed that the intracellular FFA were significantly increased, on average by 65.7% (*$P<0.05$), in LPL-OV cells compared with the control C2-GEO cells (Figure 14e). In addition, there was a highly significant increase in TG levels on average by 176.4 %(**$P<0.005$) in the LPL-OV cells (Figure 14f).

## FIGURE 14

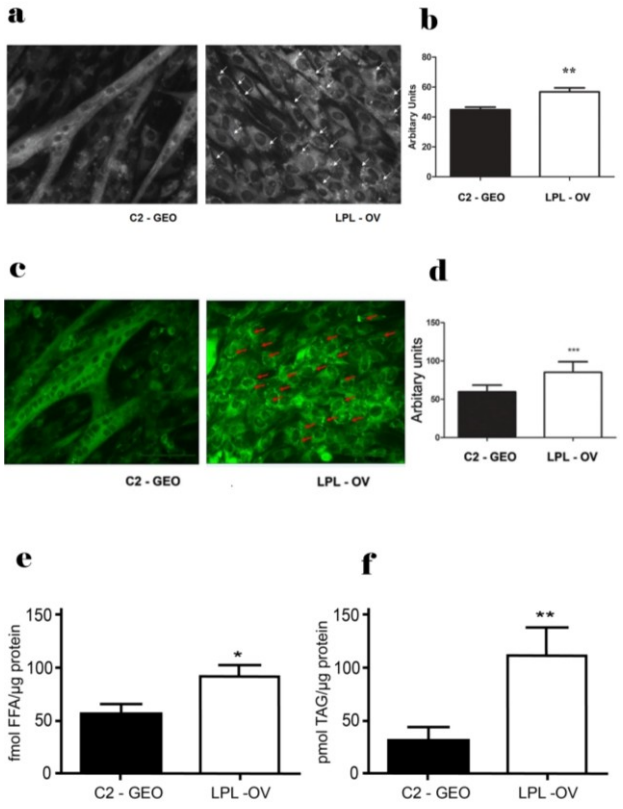


**Figure 14 a** The LPL-OV and C2-GEO cells were cultured under identical culture conditions on coverslips for microscopic analysis. The cells were stained with Nile red staining to visualize the lipids. Areas with Nile red-positive lipid droplets (indicated by white arrows) were observed exclusively in LPL-OV cells. Representative images are shown. This experiment was performed and analysed by Hannes Temmel from the group of Univ. Prof. Dr. Gerald Hoefler, Institute of Pathology at Medical University of Graz. **b** Quantification of stained cells was performed using image J. LPL-OV cultures showed significantly enhanced lipid accumulation compared to C2-GEO cells (**P<0.005). **c** Themyogenically differentiated LPL-OV and C2-GEO cells at day 6 of differentiation were stained with bodipy (neutral lipid stain). Representative images are shown. The Bodipy positive areas are indicated by red arrows. **d** Quantification of brightly stained lipid accumulating cells was performed using image J. LPL-OV cultures showed significantly more stained cells compared to C2-GEO cultures(P<0.0001). **e** FFA levels were estimated in LPL-OV and control C2-GEO cells that had been serum starved for 6 h on the 6$^{th}$ day of myogenic differentiation. The LPL-OV cells showed significantly more FFA than wt cells (92.49±10.24 fmol/µg versus 55.81±9.16 fmol FFA/µg protein, *P<0.05, n=3). **f** TheTG was measured in the same samples used to measure FFA from the myotube (6 days myogenically differentiated). The TG showed a significant increase in LPL-OV cells compared with C2-GEO cells (111.0±27.34 pmol TG/µg protein versus 30.68±12.65 pmol/µg, **P<0.005, n=3). The FFA and TG presented as mean±SD.This experiment was performed and analysed by Hannes Temmel from the group of Univ. Prof. Dr. Gerald Hoefler, Institute of Pathology at Medical University of Graz.

## *Establishing doxycycline regulated lipid overload to the C2C12 cells by hLPL, and studying its lipotoxic effects after C2C12 differentiation.*

### Construction of the clone with the hLPL gene to the Tet-on expression plasmid

The studies on LPL mediated lipotoxic effects showed the poor differentiation of LPL-OV C2C12 cells. In order to understand the lipid overload effects of C2C12 cells after differentiation, it was necessary to develop an *in vitro* cell culture model which can control the lipid uptake by an activator. To develop the cell culture model with controlled expression of hLPL in C2C12 cells, gene cloning technology was used. The schematic diagram in Figure 15 shows the generation of the clone using the hLPL gene with Tet-On expression system from Clontech. Two plasmids are used to make the clone, one is pRetro X-Tet-On Advanced, the other one is the pRetro X-Tight-Pur (Figure 15a and 15b). The hLPL mini gene coupled to a green florescent protein was isolated using a Cla1/EcoRV digest and ligated into the pRetro X-Tight-Pur (Figure 15c and 15d). The clone was created and analyzed for the right orientation using the Hind III restriction enzyme and gel electrophoresis. The gel electrophoresis results indicated the supportive plasmid and the construct plasmid with the insert in correct orientation, which was subsequently used to create stable C2C12 cells with inducible hLPL in the presence of dox.

**FIGURE 15**

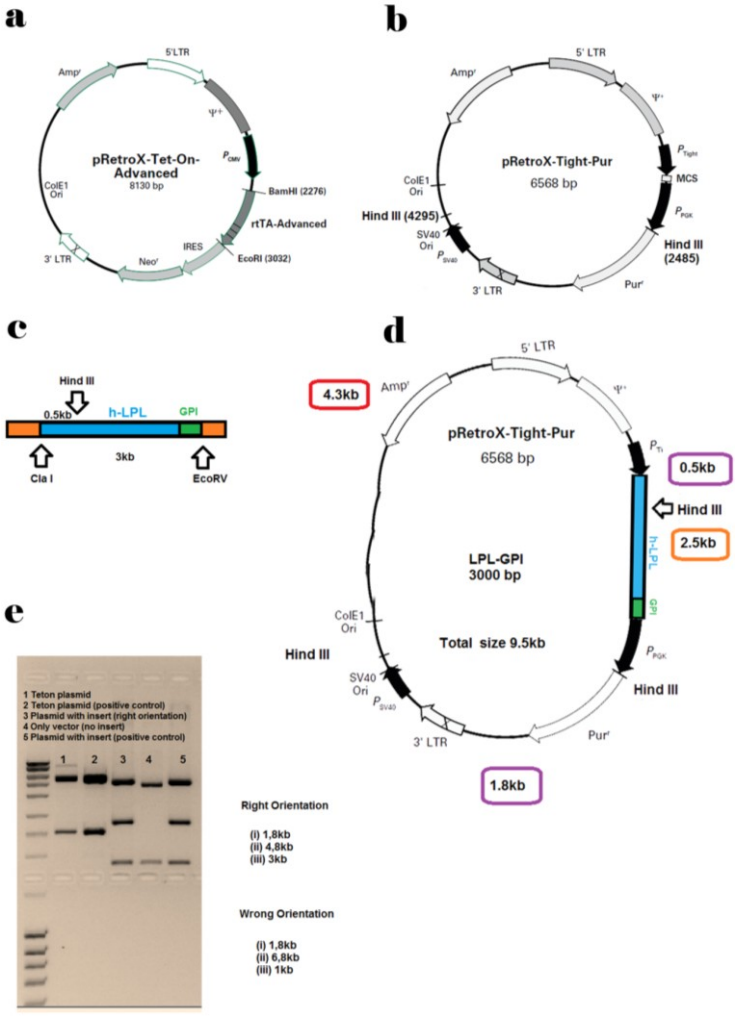


**Figure 15 a** Plasmidof pRetro X-Tet-On Advanced necessary for induction. **b** Plasmid Retro X-Tight-Pur used to insert the mini LPL-GPI gene. **c** Shows the LPL-GPI mini gene which was isolated with a Cla1/EcoRV digest. **d** Diagram of LPL-GPI gene cloned to the expression plasmid. **e**The right orientation was confirmed by using Hind III. Plasmids containing LPL-GPI in the right orientation yielded fragments of 1,8kb, 4,8kb, and 3kb size. Lane 1 and 2 in the gel picture indicate the pRetro X-Tet-On Advanced plasmid, and lane 3 and 5 indicate the LPL-GPI inserted in the right orientation in the pRetro X-Tight-Pur plasmid. Plasmid from lane 3 was used to create the stable C2C12 cells with doxycycline inducible expression of hLPL.

**The C2C12 LPL-GPI cells showed myotube differentiation.**

The C2C12 cells, with regulated expression of h-LPL under the control of doxycycline (dox) were created. Around 30 clones of LPL-GPI C2C12 cells were created and tested for the mRNA of hLPL expression after induction with 0.5µg doxy for 24 hours and without dox. The best clone was used to study the regulated lipotoxic effects of over expression of hLPL in C2C12 cells. hLPL expression was induced with 0.5µg of dox in LPL-GPI C2C12 cells during all six days of differentiation. Cells were stained with anti-MyHC antibody, followed by immunofluorescence detection to visualize myotubes (green channel) and nuclei (stained with DAPI; blue channel). Representative images are shown in Figure 16a. The IHC of the anti-MyHC indicated that there was no difference in the myotube formation between the dox regulated LPL-GPI cells compared to the control Wt cells. The TG was measured at the $6^{th}$ day of differentiation in LPL-GPI cells and control Wt cells. Results indicated that there is no significant difference in the TG level between doxy regulated LPL-GPI cells and control Wt cells (Figure 16b). In order to find the differentiation response on the $6^{th}$ day of differentiation LPL-GPI cells and control Wt cells were analyzed for MyoD expression. The relative mRNA expression results indicated no significant difference between the doxy regulated LPL-GPI and control Wt cells (Figure 16c).

## FIGURE 16

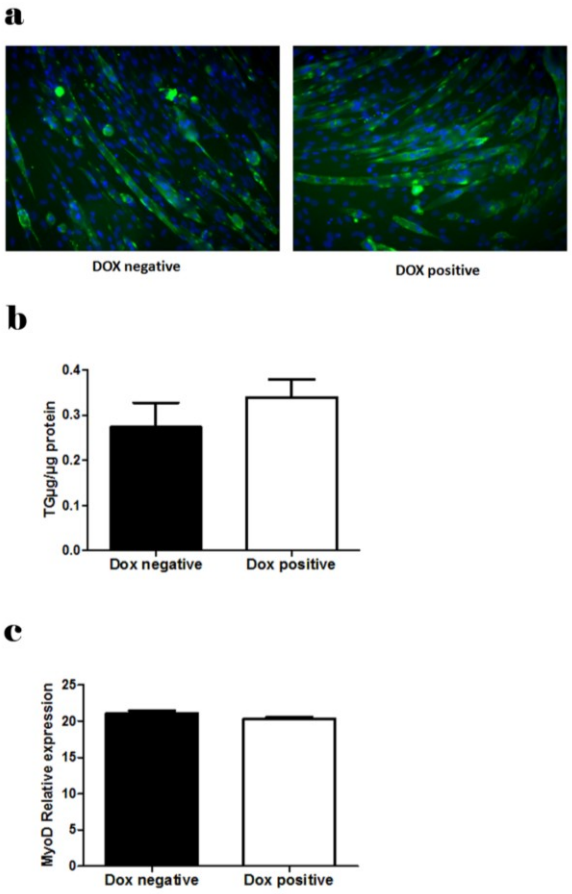


**Figure 16 a** The doxycycline treated (dox positive cells) and untreated cells (dox negative cells) after differentiation were analyzed for MyHC by IHC. Representative images showed no difference between dox positive and dox negative cells. **b** On day 6 of differentiation dox positive and dox negative cells were analyzed for the TG content. No significant differences in the TG levels between doxycycline induced and untreated cells were observed. **c** The relative expression of the MyoD in dox positive and dox negative cells showed no significant difference.

## *ATGL knockout led to the increase in the tumor growth in vivo.*

**The cell proliferation of Atgl-ko and Wt B-cells were similar under in vitro condition.**

To explore the role of Atgl related to tumor growth, B-cell derived Atgl-ko and control tumor cells were used. Six clones Atgl-ko and three clones of Wt cells were created and tested for proliferation by enumerating the cells by CASY count every day for four days. The cell proliferation studies indicated that there is no significant difference in the growth between Atgl-ko and Wt cells (Figure 17a). The Atgl-ko cells should indicate the poor expression of Atgl. Randomly selected three clones of ATGL-ko and Wt cells were analyzed of Atgl mRNA expression. The results from the three clones of both the groups indicated that the relative expression of Atgl was significantly lower in Atgl-ko than in control Wt cells (Figure 17b).

**FIGURE 17**

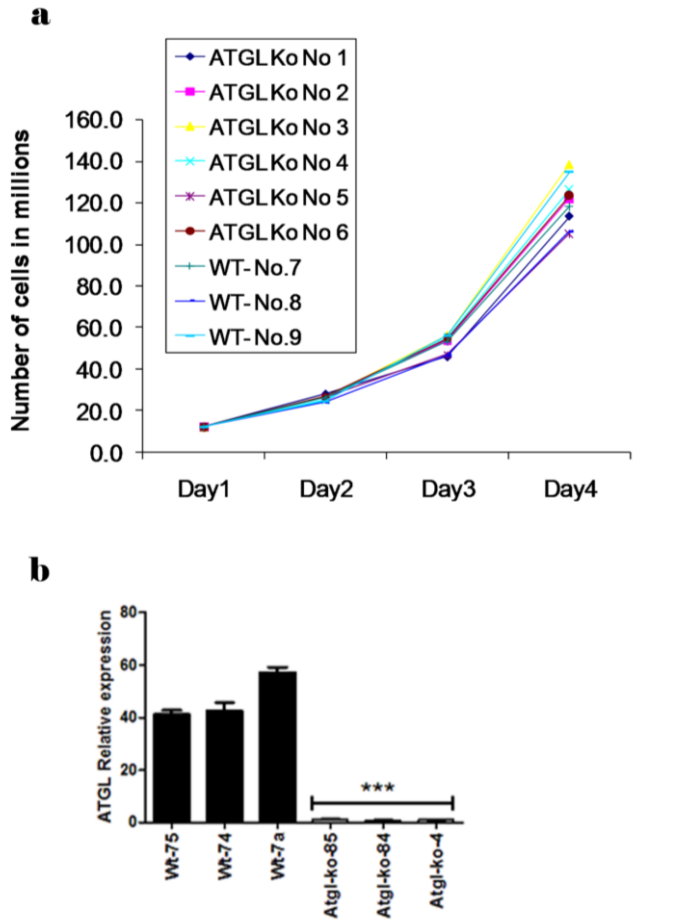


**Figure 17 a** Counting the number of Atgl-ko and wt cells for four consecutive days by CASY count revealed no significant difference between the two phenotypes with respect to proliferation. **b** The mRNA expression of Atgl from the Atgl-ko and wt cells by qRTPCR (n=3). The ATGL expression of all the three clones of Atgl-ko cells was significantly lower compared to the one of all three clones of Wt cells($p$= 0.0001). The Y axis is indicating the means ± s.e.m. The relative expression of ATGL was normalized to 18s ribosomal RNA. Statistical significance was tested using one way ANOVA, performed in Graphpad Prism version 5.

## *Atgl-ko cells showed earlier tumor formation than Wt cells in control mice*

### Atgl-ko cells tumor with various cell number and duration

In order to study tumor growth *in vivo*, Atgl-ko and wt cells were injected into mice with various cell numbers ($10\times10^5$, $5\times10^5$ and $1\times10^5$ cells) and tumor growth was determined after different periods of time. In all three groups Atgl-ko cells grow faster compared to Wt cells. The representative images of Atgl-ko and Wt tumor are indicated in the Figure 18a. After 16 days mice injected with $1\times10^5$ cells developed tumors with approx. 2 grams for Atgl-ko cells (n=3) and less than 0.5 grams for control cells (n=3, but 2 mice did not develop a tumor, Figure 18b). Mice injected with $5\times10^5$ cells developed an Atgl-ko cell tumor with approx. 1.7 grams (n=3) compared to no tumor formation with control cells (n=3) after 13 days (Figure 18c). After 13 days, mice injected with $1\times10^6$cells showed Atgl-ko cell tumors with approx. 2 grams (n=3) compared to control cell tumors with less than 0.5 grams (n=3, but 2 mice did not grow tumor, Figure 18d). Based on these results we decided to use $1.5\times10^5$cells and a period of time of 14 days for tumor growth. All three clones of Atgl-ko and wt cells ($1.5\times10^5$cells) were injected into the Wt mice, and tumor weight was determined after 14 days. The results indicated that all the three clones of Atgl-ko cells grow significantly faster than the control cells (Figure 18e).

**FIGURE 18**

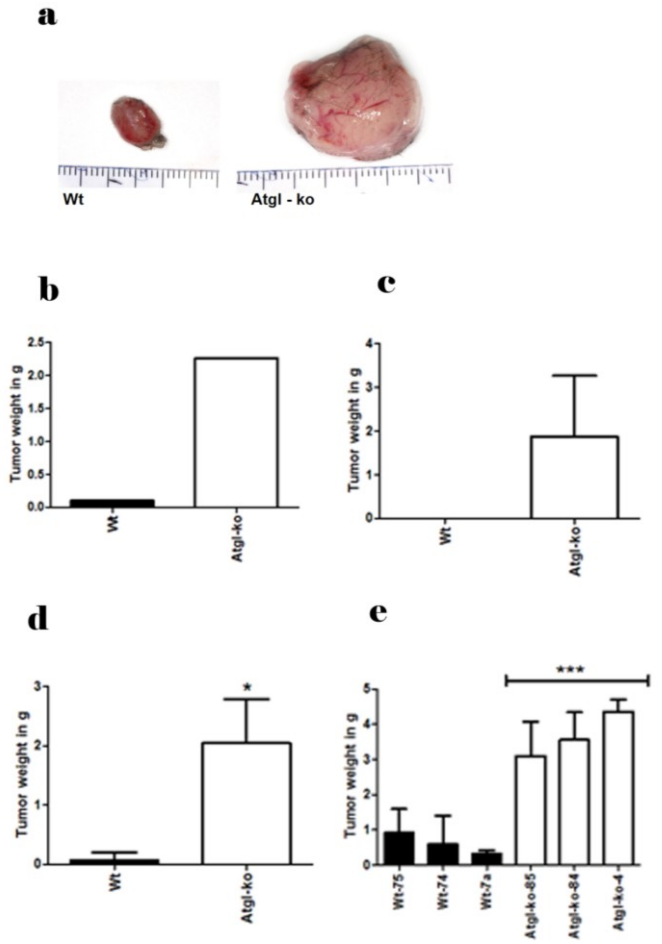


**Figure 18 a** Representative image of Atgl-ko and Wt tumor showing that the Atgl-ko cells form bigger tumors than Wt cells in Wt mice. **b** Mice were injected with $1\times10^5$ cells, and the tumor was isolated after 16 days. The Atgl-ko cell tumors weighed around 2 grams (n=3) compared to control cell tumors with less than 0.5 grams (n=3, but 2 mice did not grow tumor). **c** Mice were injected with $5\times10^5$ cells, and the tumor was isolated after 13 days. Atgl-ko cell tumors weighed around 1.7 grams (n=3) compared to control cells that developed no tumors (n=3). **d** Mice were injected with $10\times10^5$cells and the tumor was isolated after 13 days. Atgl-ko cell tumors weighed approx. 2 grams (n=3) compared to control cell tumors with less than 0.5 grams (n=3, but 2 mice did not grow tumor). **e** All three clones of Atgl-ko and wt cells ($1.5\times10^5$cells) were injected into Wt mice, and tumors were isolated after 14 days. All three clones of Atgl-ko cells grew significantly faster than control cell tumors.

**LLC-Atgl-kd cells grow bigger tumors than LLC-Atgl-wtcells**

Atgl-ko B-cells showed significantly higher tumor weight compared to Wt B-cells. For further confirmation of the role of Atgl in tumor proliferation, LLC cells with silenced Atgl (Atgl shRNA) were used to strengthen the previous findings. LLC cells with ATGL-kd and control LLC cells were injected into the flank of Wt mice and the tumors were isolated and the weight measured after 14 days. ATGL-kd LLC cells lead to significantly increased tumor weight of average 2.5 grams($p<0.0029$)compared to control LLC cells of average 1.1 grams(Figure 19 a).

**Atgl-ko tumor growth in the various mice**

In order to elucidate the role of Atgl-ko related to the gender of the mice, B-cell derived Atgl-ko and Wt cells ($1.5\times10^5$cells) were injected into male and female mice, and the tumor was isolated and weighed after 14 days. Atgl-ko cells form significantly bigger tumors in male (average 3 grams, ($p<0.0032$)) as well as in female (average 3.7 grams,($p<0.036$)) compared to Wt cells (average 0.3 grams for male and 0.4 grams for female Wt mice) (Figures 19b). To explore the role of Atgl in tumor growth related to PPAR$\alpha$ signaling, the B-cell derived ATGL-ko and Wt cells($1.5\times10^5$cells) were injected into the mice. To activate PPAR$\alpha$ signaling mice were treated with fenofibrate supplemented food. Tumors were isolated after 14 days. Atgl-ko cells grow faster in fenofibrate fed mice (average 1.7 grams ($p<0.11$)) as well as mice fed with normal chow (average2.8 grams ($p<0.02$)) compared to Wt cells (average 0.39 grams fenofibrate fed and average 0.88 grams normal chow) in Wt mice (Figures 19c).To study the immune response to Atgl-ko tumor B-cell derived Atgl-ko and Wtcells($1.5\times10^5$cells) were injected into RAG2 and RAG2 gamma mice. The tumors were isolated after 14 days and the weight was measured. Atgl-ko cell tumors grow significantly faster RAG2 mice (average 3.1 grams ($p<0.0001$) as well as in RAG2 gamma mice average 3 grams ($p<0.0001$) compared to Wt cells (average 0.47 grams RAG2 mice and 1.7 grams RAG2 gamma mice) (Figures 19e, Figures 19d).

In order to find out whether lack of Atgl in the recipient animal affects tumor growth, the B cell derived Atgl-ko and Wt cells ($1.5\times10^5$cells each) were injected into Atgl-ko mice. The tumor was isolated after 14 days and the tumor weight

measured. Atgl-ko cell tumors grew significantly faster (average 4.3 grams ($p<0.015$)) than Atgl wt tumors (average 1.1 grams) (Figure 19f).

**FIGURE 19**

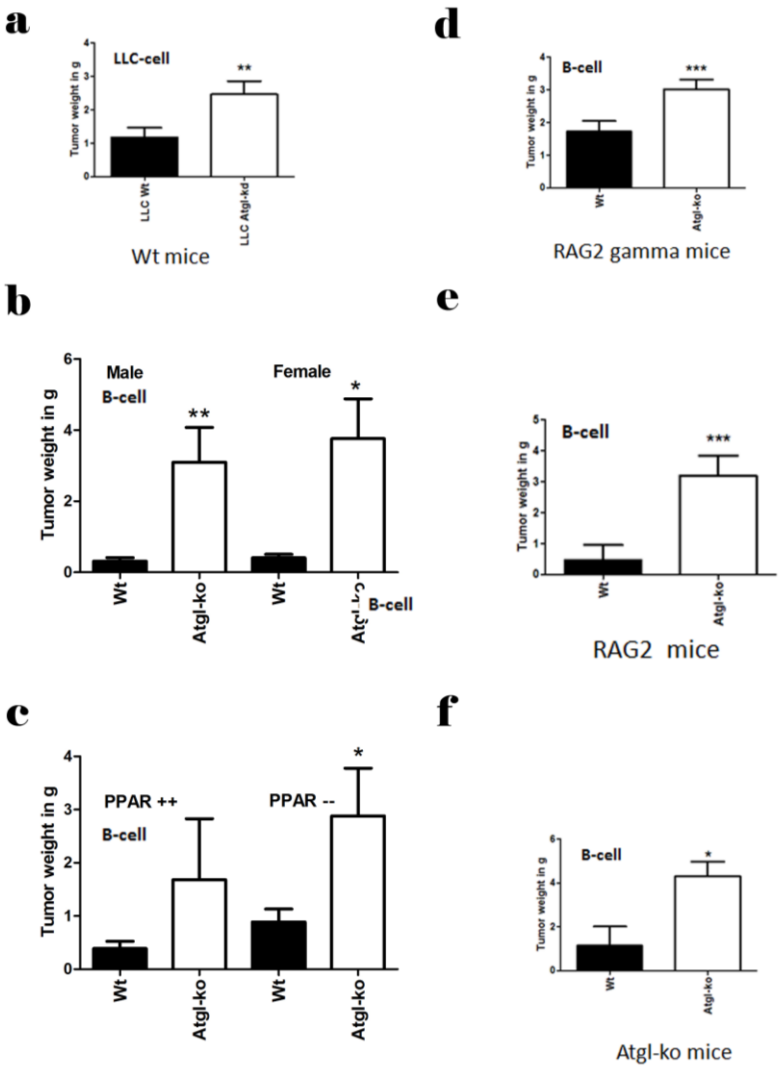


**Figure 19 a** Mice(age=36-40weeks) were inoculated in the flank with LLC-ATGL-kd cells ($2.5\times10^6$cells) and LLC-WT cells ($2.5\times10^6$cells). Tumors were isolated after 18 days and the weight measured. Tumor weight in grams of + SEM is given on the Y axis. Atgl-kd cells showed significantly increased tumor weight (2.46±0.19 grams versus 1.16±0.13 grams, **P<0.0029, n=4) compared to WT cells in mice. **b** Male mice (age=36-40 weeks) were inoculated in the flank by ATGL-ko cells and WT cells ($1.5\times10^5$cells each). The tumors were isolated after 14 days and tumor weight was determined. Tumor weight in grams + SEM is given on the Y axis. Atgl-ko cells showed significantly increased tumor weight (3.1±0.43 grams versus 0.31±0.04 grams, **P<0.0029, n=5)compared to the tumor weight from WT cells). Similarly, tumor weight from Atgl-ko cells was significantly higher compared to the one of WT cell tumors in female mice, too (3.8±0.65 grams versus 0.41±0.06 grams, *P<0.0357, n=3). **c** The normal Wt mice (age=36-40 weeks) were inoculated in the flank with ATGL-ko cells and WT cells ($1.5\times10^5$cells each). The mice were treated with PPAR agonist fenofibrate via the food. After 14 daysthe tumors were isolated and the weight

measured. The weight of Atgl-ko cell tumors was higher (1.7±0.57 grams versus 0.39±0.06 grams, P<0.1112, n=4) compared to the Wt cell tumors, and the mice treated without fenofibrate showed significantly higher weight (2.8±0.44 grams versus 0.89±0.12 grams, *P<0.0234, n=4) for Atgl-ko cell tumors compared to Wt cell tumors. **d** TheRAG2 mice gamma (age=36-40 weeks) were inoculated in the flank with ATGL-ko cells and Wt cells ($1.5\times10^5$cells each). After 14 days tumors were isolated and the weight measured. Atgl-ko cell tumors showed significantly increased tumor weight (3.02±0.12gramsversus 1.72±0.13 grams, ***P<0.0001, n=6) compared to WT cell tumors. **e** The RAG2 mice (age=36-40 weeks) were inoculated in the flank with ATGL-ko cells and WT cells ($1.5\times10^5$cells each). After 14 days tumors were isolated and the weight was measured. The Atgl-ko cell tumors showed significantly higher tumor weight (3.19±0.27 grams versus 0.47±0.21 grams, ***P<0.0001, n=5) compared to WT cell tumors. **f** Atgl-ko mice (age=36-40 weeks) were inoculated in the flank with ATGL-ko cells and WTcells ($1.5\times10^5$cells each). After 14 days tumors were isolated and the weight measured. Atgl-ko cell tumors showed significantly higher tumor weight (4.31±0.38grams versus 1.15±0.50 grams, *P<0.0153, n=3) compared to WT cell tumors.

## *Tumors from Atgl-ko cells showed altered expression of various genes compared to tumors from Atgl-wt cells.*

Our results indicated that the proliferation was comparable between Atgl-ko cells and control cells under *in vitro* culture conditions. We speculate that the tumor derived from Atgl-ko cells grew faster compared to tumors from control cells because of host-tumor interactions. For getting a better understanding about genes involved in tumor proliferation microarray analysis was performed. ATGL-ko cells and WT cells ($1.5\times10^5$cellsper mouse) were injected into the flank of BL-6 mice. Tumor growth was accessed every day and the tumor was isolated on different days in order to get tumors of similar size (Figure 20a).RNA was isolated from the ATGL-ko and Wt tumor, and tested for mRNA expression using the Affymetrix chip. The tree chart of correlative gene expression indicates the difference in the gene expression between the ATGL-ko and Wt groups (Figure 20b). In addition, there are many genes of mRNA which were up regulated (166 genes) and down regulated (454 genes) in the ATGL-ko compared to Wt tumors (data not shown). In order to validate the Affymetrix chip result, ATGL-ko cells and WT cells ($1.5\times10^5$cells/mouse) were injected into mice. Similar to the previous experiment, the tumors were isolated on different suitable days to equalize size and weight (Figure 21a).The gene expression of Caveoline2 and IRS was analyzed by qRT PCR and the results matched with the Affymetrix chip results. Caveoline2 and IRS mRNA expression was significantly higher in the ATGL-ko tumor (Figure 21b,Figure 21c).

## FIGURE 20

**a**

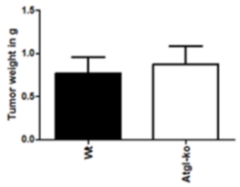


**b**

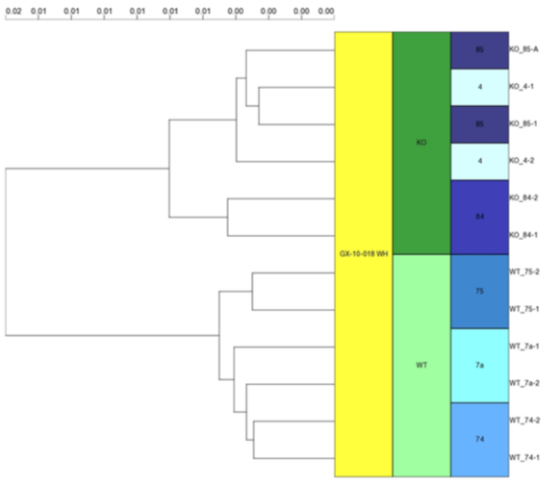


**Figure 20 a** ATGL-ko cells and WT cells ($1.5\times10^5$cells / mouse) were injected into flank of normal mice. Tumor growth was accessed every day, and the tumor was isolated on different days to get similar tumor weight (0.88±0.08grams versus 0.77±0.07 grams, P<3608, n=6). The graph indicates that the ATGL-ko and Wt tumors were similar in weight. **b** The RNA was isolated from the ATGL-ko and Wt tumor, and analyzed for mRNA expression of various genes by the Affymetrix chip. Graph shows the tree chart of correlative gene expression indicating that the ATGL-ko and Wt groups have distinguishable differences in their gene expression.

**FIGURE 21**

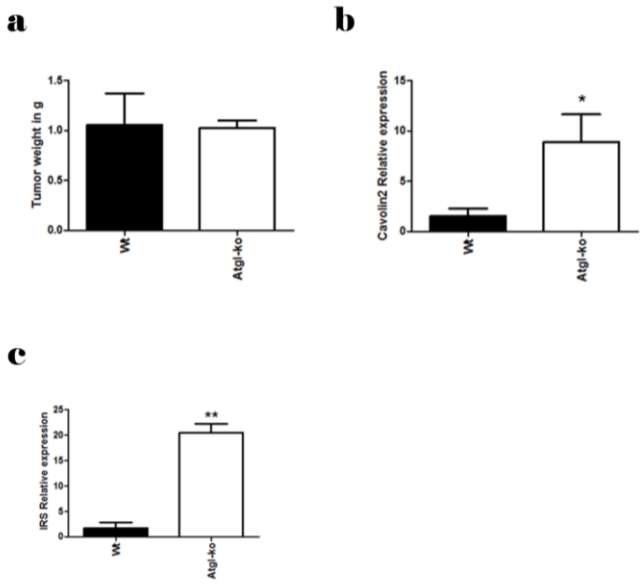


**Figure 21 a** ATGL-ko cells and WT cells ($1.5\times10^5$cells / mouse) were injected to mice. Tumors were isolated on different days to get similar tumor size and weight (1.03±0.04gversus 1.05±0.23 g, P<9338, n=3). The graph showed that the difference in weight of the ATGL-ko and Wt tumors were not significant. RNA was isolated from the ATGL-ko and Wt tumor. **b** Caveolin mRNA expression was significantly higher in ATGL-ko tumor compared to Wt tumor (8.9±1.59 relative expression versus 0.77±0.07 relative expression*P<0.0483, n=3). **C** The IRS mRNA expression was also significantly higher in ATGL-ko tumor compared to Wt tumor (20.48±1.04 relative expression versus 1.73±0.73 relative expression**P<0.0046, n=3).

.

# Discussion

Patients with cancer often undergo a specific loss of skeletal muscle mass. This condition is known as cachexia, which reduces the quality of life. In addition, loss of skeletal muscle protein contributes significantly to cancer morbidity and mortality. (Sullivan-Gunn *et al.*, 2011; Tisdale, 2001).Lipid storage myopathy is pathologically characterized by prominent lipid accumulation in muscle fibers due to lipid dysmetabolism (Liang *et al.*, 2011), and myopathies due to abnormalities in fatty acid oxidation fall into several clinical categories (Carroll, 1988).Excessive supply of FFA may have an important role in the pathogenesis of myopathy. In obese individuals increased FFA supply is often associated with metabolic syndrome, whereas in cancer cachexia enhanced amounts of FFA are released from fat deposit, for example by cytokines released from malignant tumors(Fearon, 2011).Especially in the latter, severe myopathy may develop, drastically reducing the quality of life of affected individuals (Tisdale, 2002) In order to develop rational concepts for therapeutic intervention, it is necessary to understand the pathogenic mechanisms that cause lipotoxicity in skeletal muscle. To directly investigate lipotoxicity in the skeletal muscle, the hLPL over expression models were used. Firstly, the MCK(m)-hLPL murine model system in which a human LPL mini gene that ectopically expressed under the control of the muscle-specific MCK promoter was used (Levak-Frank *et al.*, 1995). Although no systemically elevated lipid levels were found in these mice, they do show lipid overload in the muscle when kept on standard chow diet (Hoefler *et al.*, 1997; Sattler *et al.*, 1996; Voshol *et al.*, 2001).This mice model directly allows studying lipid overload in muscle (Unger *et al.*, 2010; van Herpen *et al.*, 2008). In addition another model system, the C2C12 murine myoblast cells overexpressing hLPL was used to study the lipid associated changes in myogenic potential. Finally, the new model system of hLPL gene expression in C2C12 murine myoblast under the regulation by dox was developed, and studied for its differentiation potential.

In order to analyse the mRNA expression of hLPL from MCK(m)-hLPL and control mice was analyzed by qPCR confirming strong expression of hLPL mRNA in m.gast and m.quad approximately 3 fold lower signal than18s rRNA), and inm.sol 10fold lower than 18s rRNA) of MCK(m)-hLPL mice compared to control. No

hLPL(mRNA) was detectable in Wt mice. Previous studies reported that the LPL activity was increased in 27 fold in the skeletal muscle of MCK(m)-hLPL mice (Hoefler *et al.*, 1997; Levak-Frank *et al.*, 1995; Sattler *et al.*, 1996). LPL is the central enzyme in plasma triglyceride hydrolysis, and the presence of LPL causes a myopathy and cardiomyopathy primarily by augmenting non-enzymatic selective cholesterol ester uptake (Merkel *et al.*, 2003).To study the physical performance of the MCK(m)-hLPL and the control mice, the mice were treated to run in the treadmill 10 meters per minute until a specific period. Observed result showed that endurance time in seconds of MCK(m)-hLPL mice is more than 50% reduction than the control mice. (Figure 8) In order to study the muscle weight loss in the skeletal muscle related to MCK(m)-hLPL and the control mice, all three types of muscle m.gast, m.sol, m.quad of skeletal muscles were weighed. There was a significant weight loss in the m.gast and m.quad, but no significant weight loss in m.sol(Figure 8). Earlier studies also reported that the reduction of skeletal muscle was detected both in magenetic resonsnce image analysis and macroscopic as well as microscopic pathological examination from the MCK(m)-hLPL mice (Hoefler *et al.*, 1997), but it is not reported whether it is m.gast, or m.quad or m.sol. The lack of weight loss in the m.sol might be related to the fact that hLPL expression leads to only slightly elevated level of FFA and TAG compared to m.gast. In order to investigate ultrastructural changesin m.gast and m.sol, were analyzed by electron microscopy. Irregularities of sarcomere in the m.gast of MCK(m)-hLPL mice compare to control mice were detected, but not in m.sol. This matches the loss of muscle weight because there is no difference in the m.sol weight loss between the MCK(m)-hLPL mice and control mice. Earlier studies reported that the electron microscopy of skeletal muscle of MCK(m)-hLPL mice of 5 months old mice indicated an increased number of mitochondria and severe myopathy (Levak-Frank *et al.*, 1995). Similarly a recent study showed mitochondrial alterations and oxidative stress in an acute transient mouse model of muscle degeneration, and implications for muscular dystropy related muscle pathologies (Ramadasan-Nair *et al.*, 2014).Excess of lipids in non-adipose tissue leads to cell injury which is called lipotoxicity (van Herpen *et al.*, 2008). Previous studies reported that cholesterol and triglycerides were increased in the plasma, and FFA were increased in the skeletal muscle of MCK(m)-hLPL mice compare to control mice (Levak-Frank *et al.*, 1995). m.gast and m.sol are not differentiated in

this report. FFA and TG are significantly higher in the m.gast from MCK(m)-hLPL mice compared to the control mice. m.sol of MCK(m)-hLPL mice also increased compared to the control mice, but it was less when compared to m.gast of MCK(m)-hLPL mice(Figure 9).To investigate apoptosis in skelatal muscle of MCK(m)-hLPL mice, tunnel staining, IHC of caspase, 3/7 caspase activity and the ATP protesome activity assay was tested. Skeletal muscle of MCK(m)-hLPL mice showed significantly increased caspase 3 activity. Further, IHC reativity of caspase3/7 was also significantly increased compared to control mice. Caspases are involved in apoptosis, but they are also involved in muscle differentiation and repair (Fernando *et al.*, 2002; Murray *et al.*, 2008).Therefore, terminal deoxynucleotidyl transferase dUTP nick end labeling (TUNEL) was also used to study apoptosis (Elgstrom *et al.*, 2014). M.gast of skeletal muscle from MCK(m)-hLPL mice contained significantly more tunel positive cells compared to control. Similarly, m.gast of skeletal muscle from MCK(m)-hLPL mice showed significantly increased ATP protesome activity compared to control indicating that apoptosis and protesomal activity might contribute the loss of m.gast muscle from MCK(m)-hLPL mice (Figure 10). Differences in the distribution of type IIa and type IIb fibers in gastrocnecmius and quadriceps muscles of LPL overexpressing mice and controls have been reported (Jensen *et al.*, 2008). Staining for type I and type II fibers (Figure 10) indicated no differences between hLPL transgenic and Wt mice. In these studies, type IIa and IIb fibers were not discriminated. However, it is likely that the differences reported for type IIa and IIb fibers are not sufficient to explain the severe myopathy observed in these animals. Skeletal muscle is a highly regenerative tissue and it remains somewhat surprising that the observed rate of apoptosis and proteasome activation would be sufficient to cause this rather severe phenotype. An alternative or additional explanation for this observation might relate to the fact that the regenerative potential of muscle is mainly based on the proper function of satellite cells, which are activated after muscle damage (Shi *et al.*, 2006).To study the skeletal muscle regeneration the injury was made on the tiabialis anterior muscle by cardiotoxin (CTX) injection of the MCK(m)-hLPL mice and the control mice. CTX is a peptide which was isolated from snake venoms, and it is used for skeletal muscle regeneration studies (d'Albis *et al.*, 1988). Myogenic regeneration can be characterized by the activation of myogenic cells to proliferate, differentiate, and develop new fiber formation. The regenerating fiber

was characterized by their small calibre and their centrally located myonucleai. The findings showed that regeneration of cardiotoxin induced damage from the skeletal muscle of MCK(m)-hLPL mice was reduced than the control mice(Figure 11).Further, in order to study the *in vitro* aspects of lipotoxicity to the skeletal muscle regeneration under elevated FFA and TG consequences, over expression of human lipoprotein lipase(hLPL) in the C2C12 skeletal muscle cells were used. The proliferation of LPL-OV and control C2-GEO skeletal muscle cells were analysed. The proliferation results indicated that both the LPL-OV and control C2-GEO showed similar growth (Figure 12). Once both the cells groups undergo differentiation, the LPL-OV differentiated significantly poor when compared to control C2-GEO cells (Figure12). Indeed, the LPL activity was significantly increased in the LPL-OV and control C2-GEO (Figure 13). Previous studies showed that the stable transfected hLPL in C2C12 cells increased LPL activity (Capell *et al.*, 2010), but no studies about the differentiation related to hLPL on those cells was reported. Differentiation markers proteins were identified early, and it plays role in the C2C12 differentiation (Narashimhan *et al.*, 2014). One of differentiation marker MyoD mRNA was estimated by qRT PCR, and determined to be down regulated in the LPL-OV cells (Figure 13). Very recent studies reported that the nuclear erythroid-2-p45-related factor-2(Nrf2) deficiency promotes apoptosis, and impairs MyoD expression in aging skeletal muscle cells (Narashimhan *et al.*, 2014). Lipid staining analysis on LPL-OV cells by staining as well as free fatty acid and TG measurement conclude that the excess of lipids might be involved in poor differentiation of LPL-OV cells. Previous studies showed that carnitine deficiency of human skeletal muscle is associated with lipid storage myopathy, and lipids are involved in myopathy (Engel*et al.*, 1973; Liang *et al.*, 2011). As the LPL-OV cells were differentiation poorly, C2C12 cells with hLPL expression was regulated by dox was created and tested for the differentiation. Over expression of hLPL did not inhibit C2C12 differentiation. This might be because the induction of TG by the 0.5µg of dox induced hLPL C2C12 cells was not significant(Figure 16) compared to control C2C12 cells (dox minus treatment). These studies conclude that the excess of lipids are likely to be involved in the poor differentiation of skeletal muscle cells that leads to weight loss of muscle and causes myopathy. Lipids have been reported to play a major role in myopathy (Carroll, 1988; Engel *et al.*, 1973; Liang *et al.*, 2011).Recent studies showed that

the subclinical myopathy in a child with neutral lipid storage disease and mutations in the ATGL gene (Fiorillo *et al.*, 2013). Similarly another studies showed the metabolic consequences of ATGL deficiency in humans: an *in vivo* study in patients with neutral lipid storage disease with myopathy (Natali *et al.*, 2013). Addressing the skeletal myopathy is very important because very recent studies indicating that the pathophysiology of human heart failure is related to the importance of skeletal muscle myopathy and reflexes, and the novel mechanisms emerges which contributes of skeletal muscle myopathy to heart failure. (Chapleau, 2014; Piepoli *et al.*, 2014).

To explore the role of ATGL in tumor, wildtype (Wt) and syngenic ATGL knockout (ko) tumor cells was used. The B-cell derived tumor cells, generous gift from Prof.Veronica Sexl, were created by transducing p185bcr-abl in B-cells derived from bone marrow of Wt and Atgl-ko mice. The Bcr/Abl induced Atgl-ko and Wt tumor cells were used to study the effects of inhibition of ATGL lipolysis in tumors. When the growth characteristics were analysed during *in vitro*, ATGL-ko tumor cells showed similar proliferation characteristics. *In vivo* experiments, however, demonstrated significantly increased growth rates of Atgl-ko cells compared to Wt. No gender related differences were observed since Atgl-ko tumor bigger than the Wt tumor both in male and female mice . PPARα is a one of important regulator of lipid metabolism but also plays a key role in modulating the inflammatory response in various tissues, and it is used to treat hyperlipidemic disorders (Chinetti *et al.*, 2000; Forman *et al.*, 1997). Recent studies indicated that the tumor suppression is mediated by PPARα agonists in various types of tumors (Peters *et al.*, 2012). In order to study the PPARα activation related to the ATGL inhibition to tumor growth, Atgl-ko and Wt cells injected to mice fed with fenofibrate. Fenofiberate is known to stimulate PPARα activation (Willson *et al.*, 2000).ATGL-ko tumor growth was not reduced by the stimulation of PPARα. However, recent studies indicated that the stimulation of PPARαwith fenofibrate suppress the B-cell lymphoma in mice by modulating lipid metabolism (Huang *et al.*, 2013). In addition, the PPARα activation can help prevent and treat non-small lung cancer (Skrypnyk *et al.*, 2014).To study whether the inhibition of ATGL in the cancer affects the immune reaction, immune suppressed mice were used. RAG2 mice lack mature T and B lymphocytes (Shinkai *et al.*, 1992). Similarly, RAG2 gamma is a double mutant

which is completely devoid of T, B lymphocytes, and natural killer (NK) cells (Mazurier *et al.*, 1999). In both RAG2 and RAG2 gamma mutant mice increased ATGL-ko tumor growth compared to Wt tumor was detected. In addition, the whole body knockout of ATGL mice (Haemmerle *et al.*, 2006)also showed increased ATGL-ko tumor growth compared to Wt. Recent studies indicated that the whole body knockout of ATGL prevents cancer associated cachexia. However, the whole body knockout of ATGL did inhibit the tumor induced by LLC as well as B16 melanoma cells compare to Wt mice (Das *et al.*, 2011). The Role of ATGL as well as HSL lipolysis related to the tumor was unclear (Currie *et al.*, 2013), and the observed result indicated that increased ATGL-ko tumor growth was significant in various mouse conditions. To study the various patterns of gene expressions, mice were injected with ATGL-ko and Wt cells, and same size tumors was isolated and analyzed for mRNA expression The mRNA expression of cavoline2 and IRS expression was used to validate the affimetrix result. The affimetrix result showed 166 upregulated and 454 down regulated mRNA expression of ATGL-ko versus Wt tumor (data not shown).The studies on ATGL inhibition related to tumor concluded that the knock down of ATGL play very important role in tumor growth which is independent of gender as well as PPAR alpha activation. These upregulated and down regulated genes should be further studied to decipher the underling mechanism of tumor growth related to ATGL inhibition.

.

# References


Al-Saffar NM, Troy H, Ramirez de Molina A, Jackson LE, Madhu B, Griffiths JR*, et al.* (2006). Noninvasive magnetic resonance spectroscopic pharmacodynamic markers of the choline kinase inhibitor MN58b in human carcinoma models. *Cancer research***66**(1)**:** 427-434.

Alnemri ES, Livingston DJ, Nicholson DW, Salvesen G, Thornberry NA, Wong WW*, et al.* (1996). Human ICE/CED-3 protease nomenclature. *Cell***87**(2)**:** 171.

Batista MC, Welty FK, Diffenderfer MR, Sarnak MJ, Schaefer EJ, Lamon-Fava S*, et al.* (2004). Apolipoprotein A-I, B-100, and B-48 metabolism in subjects with chronic kidney disease, obesity, and the metabolic syndrome. *Metabolism: clinical and experimental***53**(10)**:** 1255-1261.

Bauer DE, Hatzivassiliou G, Zhao F, Andreadis C, Thompson CB (2005). ATP citrate lyase is an important component of cell growth and transformation. *Oncogene***24**(41)**:** 6314-6322.

Blau HM, Pavlath GK, Hardeman EC, Chiu CP, Silberstein L, Webster SG*, et al.*(1985). Plasticity of the differentiated state. *Science***230**(4727)**:** 758-766.

Brodsky IG, Suzara D, Furman M, Goldspink P, Ford GC, Nair KS*, et al.* (2004). Proteasome production in human muscle during nutritional inhibition of myofibrillar protein degradation. *Metabolism: clinical and experimental***53**(3)**:** 340-347.

Brusselmans K, De Schrijver E, Verhoeven G, Swinnen JV (2005). RNA interference-mediated silencing of the acetyl-CoA-carboxylase-alpha gene induces growth inhibition and apoptosis of prostate cancer cells. *Cancer research***65**(15)**:** 6719-6725.

Busquets S, Carbo N, Almendro V, Figueras M, Lopez-Soriano FJ, Argiles JM (2001). Hyperlipemia: a role in regulating UCP3 gene expression in skeletal muscle during cancer cachexia? *FEBS letters***505**(2)**:** 255-258.

Capell WH, Schlaepfer IR, Wolfe P, Watson PA, Bessesen DH, Pagliassotti MJ*, et al.*(2010). Fatty acids increase glucose uptake and metabolism in C2C12 myoblasts stably transfected with human lipoprotein lipase. *American journal of physiology. Endocrinology and metabolism***299**(4)**:** E576-583.

Carroll JE (1988). Myopathies caused by disorders of lipid metabolism. *Neurologic clinics***6**(3)**:** 563-574.

Chajes V, Cambot M, Moreau K, Lenoir GM, Joulin V (2006). Acetyl-CoA carboxylase alpha is essential to breast cancer cell survival. *Cancer research***66**(10)**:** 5287-5294.

Chapleau MW (2014). Contributions of skeletal muscle myopathy to heart failure: novel mechanisms and therapies. *Experimental physiology***99**(4)**:** 607-608.

Charge SB, Rudnicki MA (2004). Cellular and molecular regulation of muscle regeneration. *Physiological reviews***84**(1)**:** 209-238.

Chinetti G, Fruchart JC, Staels B (2000). Peroxisome proliferator-activated receptors (PPARs): nuclear receptors at the crossroads between lipid metabolism and inflammation. *Inflammation research : official journal of the European Histamine Research Society ... [et al.]***49**(10)**:** 497-505.

Costelli P, Tessitore L, Batetta B, Mulas MF, Spano O, Pani P*, et al.* (1999). Alterations of lipid and cholesterol metabolism in cachectic tumor-bearing rats are prevented by insulin. *The Journal of nutrition***129**(3)**:** 700-706.

Currie E, Schulze A, Zechner R, Walther TC, Farese RV, Jr. (2013). Cellular fatty acid metabolism and cancer. *Cell metabolism***18**(2)**:** 153-161.

d'Albis A, Couteaux R, Janmot C, Roulet A, Mira JC (1988). Regeneration after cardiotoxin injury of innervated and denervated slow and fast muscles of mammals. Myosin isoform analysis. *European journal of biochemistry / FEBS***174**(1)**:** 103-110.

Das SK, Eder S, Schauer S, Diwoky C, Temmel H, Guertl B*, et al.* (2011). Adipose triglyceride lipase contributes to cancer-associated cachexia. *Science***333**(6039)**:** 233-238.

Elgstrom E, Ljungberg O, Eriksson SE, Orbom A, Strand SE, Ohlsson TG*, et al.* (2014). Change in Cell Death Markers During Lu-mAb Radioimmunotherapy-Induced Rejection of Syngeneic Rat Colon Carcinoma. *Cancer biotherapy & radiopharmaceuticals*.

Engel AG, Angelini C (1973). Carnitine deficiency of human skeletal muscle with associated lipid storage myopathy: a new syndrome. *Science***179**(4076)**:** 899-902.

Fearon KC (2011). Cancer cachexia and fat-muscle physiology. *The New England journal of medicine***365**(6)**:** 565-567.

Fernando P, Kelly JF, Balazsi K, Slack RS, Megeney LA (2002). Caspase 3 activity is required for skeletal muscle differentiation. *Proceedings of the National Academy of Sciences of the United States of America***99**(17)**:** 11025-11030.

Fiorillo C, Brisca G, Cassandrini D, Scapolan S, Astrea G, Valle M*, et al.* (2013). Subclinical myopathy in a child with neutral lipid storage disease and mutations in the PNPLA2 gene. *Biochemical and biophysical research communications***430**(1)**:** 241-244.

Forman BM, Chen J, Evans RM (1997). Hypolipidemic drugs, polyunsaturated fatty acids, and eicosanoids are ligands for peroxisome proliferator-activated receptors alpha and delta. *Proceedings of the National Academy of Sciences of the United States of America***94**(9)**:** 4312-4317.

Gauthier-Rouviere C, Vandromme M, Tuil D, Lautredou N, Morris M, Soulez M*, et al.* (1996). Expression and activity of serum response factor is required for expression of the muscle-determining factor MyoD in both dividing and differentiating mouse C2C12 myoblasts. *Molecular biology of the cell***7**(5)**:** 719-729.

Gleissner B, Gokbuget N, Bartram CR, Janssen B, Rieder H, Janssen JW*, et al.* (2002). Leading prognostic relevance of the BCR-ABL translocation in adult acute B-lineage lymphoblastic leukemia: a prospective study of the German Multicenter Trial Group and confirmed polymerase chain reaction analysis. *Blood***99**(5)**:** 1536-1543.

Greenspan P, Mayer EP, Fowler SD (1985). Nile red: a selective fluorescent stain for intracellular lipid droplets. *The Journal of cell biology***100**(3)**:** 965-973.

Haemmerle G, Lass A, Zimmermann R, Gorkiewicz G, Meyer C, Rozman J*, et al.* (2006). Defective lipolysis and altered energy metabolism in mice lacking adipose triglyceride lipase. *Science***312**(5774)**:** 734-737.

Hara A, Radin NS (1978). Lipid extraction of tissues with a low-toxicity solvent. *Analytical biochemistry***90**(1)**:** 420-426.

Hatzivassiliou G, Zhao F, Bauer DE, Andreadis C, Shaw AN, Dhanak D*, et al.* (2005). ATP citrate lyase inhibition can suppress tumor cell growth. *Cancer cell***8**(4)**:** 311-321.

Heid CA, Stevens J, Livak KJ, Williams PM (1996). Real time quantitative PCR. *Genome research***6**(10)**:** 986-994.

Hoefler G, Noehammer C, Levak-Frank S, el-Shabrawi Y, Schauer S, Zechner R*, et al.*(1997). Muscle-specific over expression of human lipoprotein lipase in mice causes increased intracellular free fatty acids and induction of peroxisomal enzymes. *Biochimie***79**(2-3)**:** 163-168.

Hoelbl A, Schuster C, Kovacic B, Zhu B, Wickre M, Hoelzl MA*, et al.*(2010). Stat5 is indispensable for the maintenance of bcr/abl-positive leukaemia. *EMBO molecular medicine***2**(3)**:** 98-110.

Horsley V, Pavlath GK (2004). Forming a multinucleated cell: molecules that regulate myoblast fusion. *Cells, tissues, organs***176**(1-3)**:** 67-78.

Huang J, Das SK, Jha P, Al Zoughbi W, Schauer S, Claudel T*, et al.* (2013). The PPARalpha agonist fenofibrate suppresses B-cell lymphoma in mice by modulating lipid metabolism. *Biochimica et biophysica acta***1831**(10)**:** 1555-1565.

Jensen DR, Knaub LA, Konhilas JP, Leinwand LA, MacLean PS, Eckel RH (2008). Increased thermoregulation in cold-exposed transgenic mice overexpressing lipoprotein lipase in skeletal muscle: an avian phenotype? *Journal of lipid research***49**(4)**:** 870-879.

Kerr JF, Wyllie AH, Currie AR (1972). Apoptosis: a basic biological phenomenon with wide-ranging implications in tissue kinetics. *British journal of cancer***26**(4)**:** 239-257.

Kutsyi MP, Kuznetsova EA, Gaziev AI (1999). Involvement of proteases in apoptosis. *Biochemistry. Biokhimiia***64**(2)**:** 115-126.

Lecker SH (2003). Ubiquitin-protein ligases in muscle wasting: multiple parallel pathways? *Current opinion in clinical nutrition and metabolic care***6**(3)**:** 271-275.

Lee Y, Hirose H, Ohneda M, Johnson JH, McGarry JD, Unger RH (1994). Beta-cell lipotoxicity in the pathogenesis of non-insulin-dependent diabetes mellitus of obese rats: impairment in adipocyte-beta-cell relationships. *Proceedings of the National Academy of Sciences of the United States of America***91**(23)**:** 10878-10882.

Lettieri Barbato D, Vegliante R, Desideri E, Ciriolo MR (2014). Managing lipid metabolism in proliferating cells: New perspective for metformin usage in cancer therapy. *Biochimica et biophysica acta*.

Levak-Frank S, Radner H, Walsh A, Stollberger R, Knipping G, Hoefler G*, et al.* (1995). Muscle-specific over expression of lipoprotein lipase causes a severe myopathy characterized by proliferation of mitochondria and peroxisomes in transgenic mice. *The Journal of clinical investigation***96**(2)**:** 976-986.

Liang WC, Nishino I (2011). Lipid storage myopathy. *Current neurology and neuroscience reports***11**(1)**:** 97-103.

Lim S, Meigs JB (2013). Ectopic fat and cardiometabolic and vascular risk. *International journal of cardiology***169**(3)**:** 166-176.

Livak KJ, Schmittgen TD (2001). Analysis of relative gene expression data using real-time quantitative PCR and the 2(-Delta Delta C(T)) Method. *Methods***25**(4)**:** 402-408.

Longo UG, Franceschi F, Ruzzini L, Rabitti C, Morini S, Maffulli N*, et al.* (2009). Characteristics at haematoxylin and eosin staining of ruptures of the long head of the biceps tendon. *British journal of sports medicine***43**(8)**:** 603-607.

Mauro A (1961). Satellite cell of skeletal muscle fibers. *The Journal of biophysical and biochemical cytology***9:** 493-495.

Mazurier F, Fontanellas A, Salesse S, Taine L, Landriau S, Moreau-Gaudry F*, et al.* (1999). A novel immunodeficient mouse model--RAG2 x common cytokine receptor gamma chain double mutants--requiring exogenous cytokine administration for human hematopoietic stem cell engraftment. *Journal of interferon & cytokine research : the official journal of the International Society for Interferon and Cytokine Research***19**(5)**:** 533-541.

McMahon DK, Anderson PA, Nassar R, Bunting JB, Saba Z, Oakeley AE*, et al.* (1994). C2C12 cells: biophysical, biochemical, and immunocytochemical properties. *The American journal of physiology***266**(6 Pt 1)**:** C1795-1802.

McNally EM, Pytel P (2007). Muscle diseases: the muscular dystrophies. *Annual review of pathology***2:** 87-109.

Mead JR, Irvine SA, Ramji DP (2002). Lipoprotein lipase: structure, function, regulation, and role in disease. *J Mol Med***80**(12)**:** 753-769.

Melo JV (1996). The diversity of BCR-ABL fusion proteins and their relationship to leukemia phenotype. *Blood***88**(7)**:** 2375-2384.

Merkel M, Radner H, Greten H (2003). [Lipoprotein lipase-mediated myopathy: implications for lipid metabolism and atherogenesis]. *Medizinische Klinik***98**(12)**:** 679-684.

Mishra S, Zhang B, Cunnick JM, Heisterkamp N, Groffen J (2006). Resistance to imatinib of bcr/abl p190 lymphoblastic leukemia cells. *Cancer research***66**(10)**:** 5387-5393.

Murray TV, McMahon JM, Howley BA, Stanley A, Ritter T, Mohr A*, et al.* (2008). A non-apoptotic role for caspase-9 in muscle differentiation. *Journal of cell science***121**(Pt 22)**:** 3786-3793.

Narashimhan M, Hong J, Atieno N, Muthusamy VR, Davidson CJ, Abu-Rmaileh N*, et al.* (2014). Nrf2 deficiency promotes apoptosis and impairs PAX7/MyoD expression in aging skeletal muscle cells. *Free radical biology & medicine*.

Natali A, Gastaldelli A, Camastra S, Baldi S, Quagliarini F, Minicocci I*, et al.* (2013). Metabolic consequences of adipose triglyceride lipase deficiency in humans: an in vivo study in patients with neutral lipid storage disease with myopathy. *The Journal of clinical endocrinology and metabolism***98**(9)**:** E1540-1548.

Nielsen TS, Jessen N, Jorgensen JO, Moller N, Lund S (2014). Dissecting adipose tissue lipolysis: molecular regulation and implications for metabolic disease. *Journal of molecular endocrinology*.

Nilsson-Ehle P (1974). Human lipoprotein lipase activity: comparison of assay methods. *Clinica chimica acta; international journal of clinical chemistry***54**(3)**:** 283-291.

Nomura DK, Long JZ, Niessen S, Hoover HS, Ng SW, Cravatt BF (2010). Monoacylglycerol lipase regulates a fatty acid network that promotes cancer pathogenesis. *Cell***140**(1)**:** 49-61.

Notarnicola M, Tutino V, Caruso MG (2014). Tumor-Induced Alterations in Lipid Metabolism. *Current medicinal chemistry*.

Pelleymounter MA, Cullen MJ, Baker MB, Hecht R, Winters D, Boone T*, et al.* (1995). Effects of the obese gene product on body weight regulation in ob/ob mice. *Science***269**(5223)**:** 540-543.

Peters JM, Shah YM, Gonzalez FJ (2012). The role of peroxisome proliferator-activated receptors in carcinogenesis and chemoprevention. *Nature reviews. Cancer***12**(3)**:** 181-195.

Piepoli MF, Crisafulli A (2014). Pathophysiology of human heart failure: importance of skeletal muscle myopathy and reflexes. *Experimental physiology***99**(4)**:** 609-615.

Poirier P, Marcell T, Huey PU, Schlaepfer IR, Owens GC, Jensen DR*, et al.* (2000). Increased intracellular triglyceride in C(2)C(12) muscle cells transfected with human lipoprotein lipase. *Biochemical and biophysical research communications***270**(3)**:** 997-1001.

Ramadasan-Nair R, Gayathri N, Mishra S, Sunitha B, Mythri RB, Nalini A*, et al.* (2014). Mitochondrial alterations and oxidative stress in an acute transient mouse model of muscle degeneration: implications for muscular dystrophy and related muscle pathologies. *The Journal of biological chemistry***289**(1)**:** 485-509.

Raponi S, De Propris MS, Wai H, Intoppa S, Elia L, Diverio D*, et al.* (2009). An accurate and rapid flow cytometric diagnosis of BCR-ABL positive acute lymphoblastic leukemia. *Haematologica***94**(12)**:** 1767-1770.

Reinheckel T, Sitte N, Ullrich O, Kuckelkorn U, Davies KJ, Grune T (1998). Comparative resistance of the 20S and 26S proteasome to oxidative stress. *The Biochemical journal***335 ( Pt 3):** 637-642.

Rozen S, Skaletsky H (2000). Primer3 on the WWW for general users and for biologist programmers. *Methods in molecular biology***132:** 365-386.

Sattler W, Levak-Frank S, Radner H, Kostner GM, Zechner R (1996). Muscle-specific over expression of lipoprotein lipase in transgenic mice results in increased alpha-tocopherol levels in skeletal muscle. *The Biochemical journal***318 ( Pt 1):** 15-19.

Shi X, Garry DJ (2006). Muscle stem cells in development, regeneration, and disease. *Genes & development***20**(13)**:** 1692-1708.

Shimabukuro M, Koyama K, Chen G, Wang MY, Trieu F, Lee Y*, et al.* (1997). Direct antidiabetic effect of leptin through triglyceride depletion of tissues. *Proceedings of the National Academy of Sciences of the United States of America***94**(9)**:** 4637-4641.

Shinkai Y, Rathbun G, Lam KP, Oltz EM, Stewart V, Mendelsohn M*, et al.*(1992). RAG-2-deficient mice lack mature lymphocytes owing to inability to initiate V(D)J rearrangement. *Cell***68**(5)**:** 855-867.

Skrypnyk N, Chen X, Hu W, Su Y, Mont S, Yang S*, et al.* (2014). PPARalpha activation can help prevent and treat non-small cell lung cancer. *Cancer research***74**(2)**:** 621-631.

Soulez M, Rouviere CG, Chafey P, Hentzen D, Vandromme M, Lautredou N*, et al.* (1996). Growth and differentiation of C2 myogenic cells are dependent on serum response factor. *Molecular and cellular biology***16**(11)**:** 6065-6074.

Staber PB, Vesely P, Haq N, Ott RG, Funato K, Bambach I*, et al.* (2007). The oncoprotein NPM-ALK of anaplastic large-cell lymphoma induces JUNB transcription via ERK1/2 and JunB translation via mTOR signaling. *Blood***110**(9)**:** 3374-3383.

Sullivan-Gunn MJ, Campbell-O'Sullivan SP, Tisdale MJ, Lewandowski PA (2011). Decreased NADPH oxidase expression and antioxidant activity in cachectic skeletal muscle. *Journal of cachexia, sarcopenia and muscle***2**(3)**:** 181-188.

Swinnen JV, Brusselmans K, Verhoeven G (2006). Increased lipogenesis in cancer cells: new players, novel targets. *Current opinion in clinical nutrition and metabolic care***9**(4)**:** 358-365.

Tamilarasan KP, Temmel H, Das SK, Al Zoughbi W, Schauer S, Vesely PW*, et al.* (2012). Skeletal muscle damage and impaired regeneration due to LPL-mediated lipotoxicity. *Cell death & disease***3:** e354.

Tisdale MJ (2002). Cachexia in cancer patients. *Nature reviews. Cancer***2**(11)**:** 862-871.

Tisdale MJ (2001). Loss of skeletal muscle in cancer: biochemical mechanisms. *Frontiers in bioscience : a journal and virtual library***6:** D164-174.

Todd R, Wong DT (1999). Oncogenes. *Anticancer research***19**(6A)**:** 4729-4746.

Unger RH, Clark GO, Scherer PE, Orci L (2010). Lipid homeostasis, lipotoxicity and the metabolic syndrome. *Biochimica et biophysica acta***1801**(3)**:** 209-214.

van Herpen NA, Schrauwen-Hinderling VB (2008). Lipid accumulation in non-adipose tissue and lipotoxicity. *Physiology & behavior***94**(2)**:** 231-241.

Venable JH, Coggeshall R (1965). A Simplified Lead Citrate Stain for Use in Electron Microscopy. *The Journal of cell biology***25:** 407-408.

Voshol PJ, Jong MC, Dahlmans VE, Kratky D, Levak-Frank S, Zechner R*, et al.* (2001). In muscle-specific lipoprotein lipase-overexpressing mice, muscle triglyceride content is increased without inhibition of insulin-stimulated whole-body and muscle-specific glucose uptake. *Diabetes***50**(11)**:** 2585-2590.

Wakil SJ, Abu-Elheiga LA (2009). Fatty acid metabolism: target for metabolic syndrome. *Journal of lipid research***50 Suppl:** S138-143.

Wang HQ, Altomare DA, Skele KL, Poulikakos PI, Kuhajda FP, Di Cristofano A*, et al.* (2005). Positive feedback regulation between AKT activation and fatty acid synthase expression in ovarian carcinoma cells. *Oncogene***24**(22)**:** 3574-3582.

Welty FK, Lichtenstein AH, Barrett PH, Dolnikowski GG, Schaefer EJ (2004). Interrelationships between human apolipoprotein A-I and apolipoproteins B-48 and B-100 kinetics using stable isotopes. *Arteriosclerosis, thrombosis, and vascular biology***24**(9)**:** 1703-1707.

Willson TM, Brown PJ, Sternbach DD, Henke BR (2000). The PPARs: from orphan receptors to drug discovery. *Journal of medicinal chemistry***43**(4)**:** 527-550.

Yaffe D, Saxel O (1977). Serial passaging and differentiation of myogenic cells isolated from dystrophic mouse muscle. *Nature***270**(5639)**:** 725-727.

Young CD, Anderson SM (2008). Sugar and fat - that's where it's at: metabolic changes in tumors. *Breast cancer research : BCR***10**(1)**:** 202.

Young SG, Zechner R (2013). Biochemistry and pathophysiology of intravascular and intracellular lipolysis. *Genes & development***27**(5)**:** 459-484.

Zhang SO, Trimble R, Guo F, Mak HY (2010). Lipid droplets as ubiquitous fat storage organelles in C. elegans. *BMC cell biology***11:** 96.

Zhou YT, Shimabukuro M, Koyama K, Lee Y, Wang MY, Trieu F*, et al.* (1997). Induction by leptin of uncoupling protein-2 and enzymes of fatty acid oxidation. *Proceedings of the National Academy of Sciences of the United States of America***94**(12)**:** 6386-6390.

## Acknowledgement

I am very proud to mention that I have great satisfaction for me to express my deep sense of my guide Prof. Gerald Hoefler for the attention, guidance, intervention and encouragement provided by him for the successful completion of my PhD dissertation. I am very grateful to him for his encouragement of new ideas and support to the end required for the successful accomplishment of the project(S). I shall be always indebt to him for the financial and personal support during difficult times. I am really thankful to him for his time to discuss the results, feature plans as well as other scientific matters in and out of the lab. Sometimes, I have doubt and lack of direction. He continuously guided me and motivated me to proceed further.

I am very grateful to thank Silvia Schauer for very well planned mentor in the lab and helping me from every possible facet throughout my tenure in Austria in and out of lab. I am thankful to her for teaching me the mice experimental work and many more techniques for the successful completion of project(S). I am very glad to mention that Silvia Schauer for helping me with all the experiments and also handling the management to get the chemicals required for the experiments. I will always be grateful to her for letting me understand the value of management. I really respect her for managing the whole group like a very well planned management along with helping everyone in any every possible situation. I also would like to apologize to her for my mistakes which occurred unknowingly or forced situation based knowingly. I am very glad that she maintained her positive attitude and patience with persisted to bring the best out of scientific technical skills of me.

I was also guided by my thesis committee, namely Prof. Dagmar Kratky and Prof. Ellen Zechner who provided the basic frame work for my project but also granted help during the whole period of my PhD time schedule. I am really thankful to them for their patience in making me understand the topic and also evaluating my poor results. Their constructive criticism helped me in developing a scientific attitude to my work. I am very glad to mention that their insistence helped me to achieving

perfection and motivated me to improve my work strive hard to meet their standards

I would like to thank Prof. Gerald Hoefler and Prof. Dagmar Kratky and Prof. Ellen Zechner for reviewing, and giving direction to the research work every year as thesis committee members. Their suggestions certainly improved the thesis immensely which I can present respectfully.

I am very glad to mention that Dr. Paul Vessely for his patience and coaching me through various essential techniques to develop the cloning technology for the Teton-expressions system as well as other experiments throughout the studies, and it is the stable base for all the projects performed by me during my PhD tenure. He involved in monitoring and correcting as well as corresponding author of the scientific research and contributed up to the publish of research in the scientific journal. I would like to thank all the faculty of the PhD program Molecular Medicine for introducing me to the interesting and essential topics of medicine and natural sciences. Their comments in thesis seminars helped improving my work. I am also grateful to Hannes Teammel for his constructive criticism towards my work and his willingness to help in every possible venture taken by me.

I am very grateful to thank Univ. Prof. Dr. Veronika Sexl for providing the B-cells for the study of ATGL lipolysis related to tumor metabolism.

I very thankfull to my entire group lead by Prof. Gerald Hofler and comprising Dr. Wael Alzoughbi, Silvia Schauer, Hannes Teammel, Dr.Upeka Senanayake, Dr. Pooja Kumari, Jian Fenf, Ganapathy, Mathias Romauch, Dr. Paul Vessely, Dr. Barbara Gurtl-Lackner and Dr. Elke Stadelmeyer for providing me a very good environment which helped me in enjoying my work. Without their guidance I could have never achieved anything. I will miss the super power group meetings, numerous different parties and short excursions which allowed me enjoying the scientific life in our lab.

I am grateful to Dr. Elke Stadelmeyer for great valuable input to writing thesis making all the complicated data arrangements into simpler easier format, and guided me to handle the related softwers of word and power points as well as excel. I greatly thank her for her patient towards me whenever I confuse her with scientific as well as technical related works for the thesis.

I am grateful to Karin Osibow for handling all the complicated arrangements from the beginning including starting from the guidance of the very complicated VISA process, administrated process that made my stay feel free in new international environment. I greatly thank her for her patient towards me whenever I confuse her with many possible documents in German language. Her explanation was very simple and it is cool.

I would like to thank Medical University of Graz and the Center for medical Research (ZMF) for providing the very great research environment. I take this opportunity to thank all my friends in Graz and I also like to extend my deepest gratitude to my co-workers for giving the moral support and My parents and My brothers, who always helped me under various situation and kept me fulfilling all my demands.

**Funding**

This PhD thesis work was supported by grant F30 SFB LIPOTOX, funded by the Austrian Science Fund (FWF) and the PhD program Molecular Medicine of the Medical University of Graz.

# Declaration

I hereby declare that this thesis is my own original work and that I have fully acknowledged by name all of those individuals and organisations that have contributed to the research for this thesis. Due acknowledgement has been made in the text to all other material used. Throughout this thesis and in all related publication I followed the guidelines of “Good Scientific Practice”

# Appendix

## Year 2012

**Publication:**

**Tamilarasan KP,** Temmel H, Das SK, Alzoughbi W, Schauer S, Vesely PW, Höfler G**Skeletal muscle damage and impaired regeneration due to LPL-mediated lipotoxicity.**Cell Death Dis. 2012 Jul 19;3:e354. doi: 10.1038/cddis.2012.91.

## Year 2011

**Publication:**

Das SK, Eder S, Schauer S, Diwoky C, Temmel H, Guertl B, Gorkiewicz G, **Tamilarasan KP**, Kumari P, Trauner M, Zimmermann R, Vesely P, Haemmerle G, Zechner R, Hoefler G. **Adipose triglyceride lipase contributes to cancer-associated cachexia.**Science. 2011 Jul 8;333(6039):233-8. doi: 10.1126/science.1198973. Epub 2011 Jun 16. Erratum in: Science. 2011 Sep 16;333(6049):1576.

## Year 2010

**Poster:**

- **Tamilarasan KP**, Alzoughbi W, Das SK, Vesely PW, Schauer S, Hämmerle G, Zechner R, Sexl V and Höfler G. **Importance of ATGL in Tumor Progression.**3rd International Symposium on Lipid and Membrane Biology March 18-20 Importance of ATGL in Tumor Progression

**Poster:**

- **Tamilarasan KP**, Al Zoughbi W, Das SK, Vesely PW, Schauer S, Gürtl-Lackner B, Hämmerle G, Zechner R, Sexl V and Hoefler G. **Importance of ATGL in Tumor Progression.**November 5 & 6 Joint ZMF & Doctoral Days

## Year 2009

**Poster:**

- **Tamilarasan KP**,Temmel H,[1]Schauer S, Levak-Frank S, Eckel RH, Das S, Vesely PW & Hoefler G. ***Lipotoxicity in murine muscle cells***.November 4 & 5 Joint ZMF & Doctoral Days

**Poster:**

- **Tamilarasan KP**,Temmel H, Schauer S, Levak-Frank S, Eckel RH, Das S, Vesely PW & Hoefler G. ***Lipotoxicity in murine muscle cells***SFB Lipotox workshop April 15-16 2009.

**Publication:**

- Barbara Gu rtl, Dagmar Kratky, Christian Guelly, Lefeng Zheng, Gregor Gorkiewicz,Suman Kumar Das, **Tamilarasan, KP** and Gerald Hoefler. Apoptosis and fibrosis are early features of heart failure in an animal model of metabolic cardiomyopathy ***Int. J. Exp. Path.*** *(2009) 90,*

## Year 2008

**Poster:**

- **K.P. Tamilarasan**, Schauer S., Balint Z., Das SK., Chandran N., Temmel H., Vesely, P, Ibovnik A., Zhou Yulai, Absenger M, Novak A, Schloffer M, Gorkiewicz G., Hämmerle G., Zimmermann R., Goldberg IJ, Kratky D., Olschewski A., Zechner R.,Höfler G.**Effects of Nitric oxide inLipotoxic Cardiomyopathy**November 12 ZMF-Day